PTEP

Prog. Theor. Exp. Phys. **2023** 013D01(30 pages)
DOI: 10.1093/ptep/ptac134

Effective two-body $\Lambda N \to NN$ weak potentials deduced from three-body $\Lambda NN \to NNN$ interactions and hypernuclear non-mesonic weak decay rates

Kazunori Itonaga[1,2,⋆], Toshio Motoba[3,4,5], and Thomas A. Rijken[6]

[1]*Faculty of Medicine, University of Miyazaki, Miyazaki 889-1692, Japan*
[2]*Physics Department, Gifu University, 1-1 Yanagido, Gifu 501-1193, Japan*
[3]*Research Center for Nuclear Physics, Osaka University, Ibaraki, Osaka 567-0047, Japan*
[4]*Laboratory of Physics, Osaka Electro-Communication University, Neyagawa 572-8530, Japan*
[5]*Yukawa Institute for Theoretical Physics, Kyoto University, Kyoto 606-8502, Japan*
[6]*Institute of Mathematics, Astrophysics, and Particle Physics, Radboud University, NL-6525 ED Nijmegen, The Netherlands*
⋆E-mail: kazunori.itonaga@gmail.com

Received May 1, 2022; Revised September 23, 2022; Accepted September 30, 2022; Published October 4, 2022

We intend to study the role of the three-body weak $\Lambda NN \to NNN$ interaction in two-nucleon induced hypernuclear non-mesonic weak decay. The three-body weak interactions are constructed on the basis of the meson-pair exchange (MPE) model and then we derive the effective two-body $\Lambda N \to NN$ weak potentials from the three-body interactions based on the Loiseau–Nogami–Ross approximation. The strong coupling constants of MPE are taken from the Nijmegen ESC and GESC models and the weak ones of MPE are evaluated in the weak Λ–n mixing model by Dalitz and Von Hippel [Phys. Lett. **10**, 153 (1964)]. The effective two-body $\Lambda N \to NN$ weak potentials are applied to evaluate hypernuclear non-mesonic decay rates, which should give a certain additional contribution to the two-nucleon induced decay rate Γ_{2N}. Calculations of $\Gamma_{nm}^{(\mathrm{eff.2B})}$ are done for ${}^{5}_{\Lambda}$He, ${}^{11}_{\Lambda}$B, and ${}^{12}_{\Lambda}$C and the results are compared with experimental data $\Gamma_{2N}^{\mathrm{exp}}$. We have demonstrated the possibility of accounting for the two-nucleon induced non-mesonic decays of light and p-shell hypernuclei by introducing the effective two-body potentials deduced from the three-body weak interactions, though the calculated $\Gamma_{nm}^{(\mathrm{eff.2B})}$ still includes uncertainties. Discussions and limitations of our "effective two-body $\Lambda N \to NN$ model" are given.

Subject Index D02, D14, D29

1. Introduction

In these days the understanding of the weak decay mechanism and the decay interaction of Λ embedded in the nuclear medium has much progressed, owing to the experimental advent of innovative detection techniques and the theoretical efforts in clarifying the variety of Λ-producing decay observables adhering to hypernuclei [1–3].

A free Λ decays exclusively through the pi-mesonic modes, i.e., $\Lambda \to p\pi^-$ and $\Lambda \to n\pi^0$. However, it is also well known that once Λ has been trapped in the nucleus Λ can exhibit the new weak decay mode, i.e., non-mesonic decays such as the $\Lambda p \to np$ and $\Lambda n \to nn$ processes, in addition to the pi-mesonic decay mode. Such one-nucleon induced non-mesonic decay processes become the dominant weak decay mode for all the Λ-hypernuclei except for light s-shell systems.

Studies on one-nucleon induced decays have been done using a variety of weak interactions of $V(\Lambda N\text{–}NN)$ such as the meson-exchange (one-meson exchange, two-meson exchange, correlated or uncorrelated meson-pair exchange) models, quark exchange model, and effective field theory, etc., in combination with many-body treatments such as the shell model and/or the nuclear matter framework. The non-mesonic partial decay rates, $\Gamma_p(\Lambda p \to np)$, $\Gamma_n(\Lambda n \to nn)$, the ratio Γ_n/Γ_p, and the asymmetry parameter α_Λ for the decay protons from the polarized hypernuclei are important weak decay observables. Recent theories [4–6] seem to account for those data successfully to a certain extent, though we think that they are not yet fully understood.

However, close attention must be paid to the proton/neutron distribution and the nucleon-pair (*np* and *nn*) distributions as a function of the kinetic energy or opening angle of the pair nucleons in the final state. It has long been recognized that the nucleon and nucleon pair do not show a simple pattern originating from the one-nucleon induced decays even when one considers the final-state interactions (FSI). Alberico et al. [7] were the first to point out the possibility of such a process in which the virtual pion from the Λ decay can be absorbed by a pair of nucleons as *np*, producing three-body decays, i.e., the $\Lambda NN \to NNN$ process in nuclear matter.

Recently two groups observed the two-nucleon induced three-body decay rate $\Gamma_{2N}(\Lambda NN \to NNN)$. One is the KEK E462-E508 group, who noticed the following. Yield quenching exists both in one-nucleon energy spectra (proton and neutron) in the lower-energy part and in the nucleon-pair (*np* and *nn*) distribution for their opening angle and also for the momentum-sum in the non-mesonic decay of ${}^{12}_{\Lambda}\mathrm{C}$ with respect to those expected in the model calculations of only one-nucleon induced decay with FSI. They considered and analyzed that the quenching phenomenon could be caused by the two-nucleon induced three-body process as $\Lambda NN \to NNN$ and FSI. They obtained the two-nucleon induced decay rate $\Gamma_{2N} = 0.27 \pm 0.13\Gamma_\Lambda$ ($\Gamma_{2N}/\Gamma_{NM} = 0.29 \pm 0.13$) for ${}^{12}_{\Lambda}\mathrm{C}$ [8,9]. Γ_Λ is a free Λ decay rate. The other group is the FINUDA Collaboration, who untangled the contribution of two-nucleon induced non-mesonic decays in two ways under some assumptions: (a) analyzing inclusive decay single-proton spectra affected by FSI for $A = 5$–16 hypernuclei to extract $2N$ induced decay rates by fitting each of the proton kinetic energy spectra for their high-energy part with a Gaussian function [10] and (b) considering both proton and neutron spectra and also neutron–proton coincidence events in suitable kinematical configurations to determine Γ_{2N} [11]. The updated results [12,13] are $\Gamma_{2N}/\Gamma_{NM} = 0.25 \pm 0.12 \pm 0.02$ for method (a) and $\Gamma_{2N}/\Gamma_{NM} = 0.20 \pm 0.08^{+0.04}_{-0.03}$ for method (b). The reported values are for the average of hypernuclei of $A = 5$–16.

After the work of Ref. [7], Ramos et al. [14] applied the formalism to finite hypernuclei using the local density approximation (LDA). Bauer et al. [15–17] extended further the nuclear matter formalism microscopically by taking into account the meson-exchange weak interactions that couple to the two-particle–two-hole excitations arising from the ground-state correlation due to the strong residual interactions. They evaluated the two-nucleon induced decay rate of ${}^{12}_{\Lambda}\mathrm{C}$ by adopting the LDA in their formalism and obtained $\Gamma_{2N} = 0.26\Gamma_\Lambda$ [17]. However, the calculated Γ_{2N} looks so large that the following questions may naturally arise: (i) Is the nuclear ground-state correlation so big to produce large Γ_{2N}? (ii) Are there any ambiguities for the nuclear residual interactions?

On the other hand, Shinmura was a pioneer, thinking about the role of the three-body force on the two-nucleon induced non-mesonic decay [18]. He examined the Fujita–Miyazawa-type [19] weak three-body force in a relativistic way by incorporating the Dirac wave functions for

bound Λ and nucleons, and evaluated the decay rates of the three-body mechanism with results $\Gamma_{2N}\,(\equiv \Gamma_3)$ about 30% of the total Γ_{NM} for s-shell hypernuclei.

The motivation for this work is to understand the hypernuclear weak two-nucleon induced decay mechanism and the decay rates more deeply from a new viewpoint. This is because of the following. First, although it is stated that the one-nucleon induced decay is rather well understood, the summed decay rate $\Gamma_{NM} = \Gamma_{1N} + \Gamma_{2N}$ should be recognized more accurately, because Γ_{2N} is not settled experimentally and theoretically. Even Γ_{1N} is in principle affected by two-nucleon induced decays through FSI between the outgoing nucleons. Further, the hypernuclear lifetime is connected with Γ_{NM} and consequently with Γ_{2N} through the relation $\tau_{HY} = \hbar/(\Gamma_\pi + \Gamma_{NM})$. Secondly, as mentioned, experimental data for Γ_{2N} have been reported by two groups; the data for ${}^{12}_{\Lambda}$C from the KEK E462-E508 group still have large error bars, while the FINUDA data are determined under the assumptions of (i) a linear dependence of the FSI contribution on A and (ii) the constancy of both Γ_n/Γ_p and Γ_{2N}/Γ_{NM} for $A = 5$–16 hypernuclei. We would expect a more improved and direct determination of Γ_{2N} along with the experimental progress. On the theoretical side, there is a fundamental problem with the two-nucleon induced non-mesonic weak decay. What is the dominant and relevant mechanism for two-nucleon induced decays? This is not fully discussed and clarified theoretically. We would like to explore the two-nucleon induced weak decay with a different approach; i.e., we propose that the $\Lambda NN \to NNN$ three-body weak interaction is dominantly responsible for the two-nucleon induced weak decay. This view is different from the polarization propagator method (PPM) approach developed by Ramos et al. [14] and Bauer et al. [15–17]. The mechanism of the two-nucleon induced decay of PPM is that a meson emitted in the two-body weak $\Lambda N \to NN$ transition interacts with a particle or a hole in the two-particle–two-hole excitations in the ground-state correlation due to the residual strong NN–NN interactions in the nuclear matter and finally the three nucleons are emitted. Our method has the advantage of evaluating the non-mesonic weak decay rates for finite hypernuclear systems in terms of the parent hypernuclear and daughter nuclear wave functions.

In this paper we try to evaluate the two-nucleon induced non-mesonic decay rate by a new approach. We consider two mechanisms. One process is that a virtual meson emitted from Λ in the weak process is absorbed by the first nucleon; it then emits simultaneously (at the same space-time position) another meson that is finally captured by the second nucleon. The second process is that Λ emits a meson pair in the weak process and the emitted two mesons are captured by two different nucleons. These two processes can be regarded as the three-body interaction mechanism of Λ–nucleon–nucleon going to three nucleons mediated by the meson-pair exchange (MPE) as shown in Fig. 1. In the MPE, we consider the $(\pi\sigma)$, $(\pi\omega)$, and $(\sigma\sigma)$ exchanges, and in addition the Fujita–Miyazawa-type $(\pi\pi)$ exchange. It should be noted, however, that the full treatment of the weak three-body interaction in the weak decay of Λ-hypernuclei in the wave function formalism is too complicated at present. Instead, here we transform the weak three-body interaction to the "effective" two-body $\Lambda N \to NN$ weak potential by integrating the "third" particle in the three-body interaction. Thus the effective two-body $\Lambda N \to NN$ weak potentials deduced from the three-body interactions have a different nature from the usual two-body weak $\Lambda N \to NN$ potentials. Therefore we treat the "effective" two-body potentials separately from the usual two-body ones in evaluating hypernuclear decay rates.

In Sect. 2, we show three-body weak interaction processes on the basis of the meson-pair exchange model of the Nijmegen ESC model. In Sect. 3, we explain how to construct effective

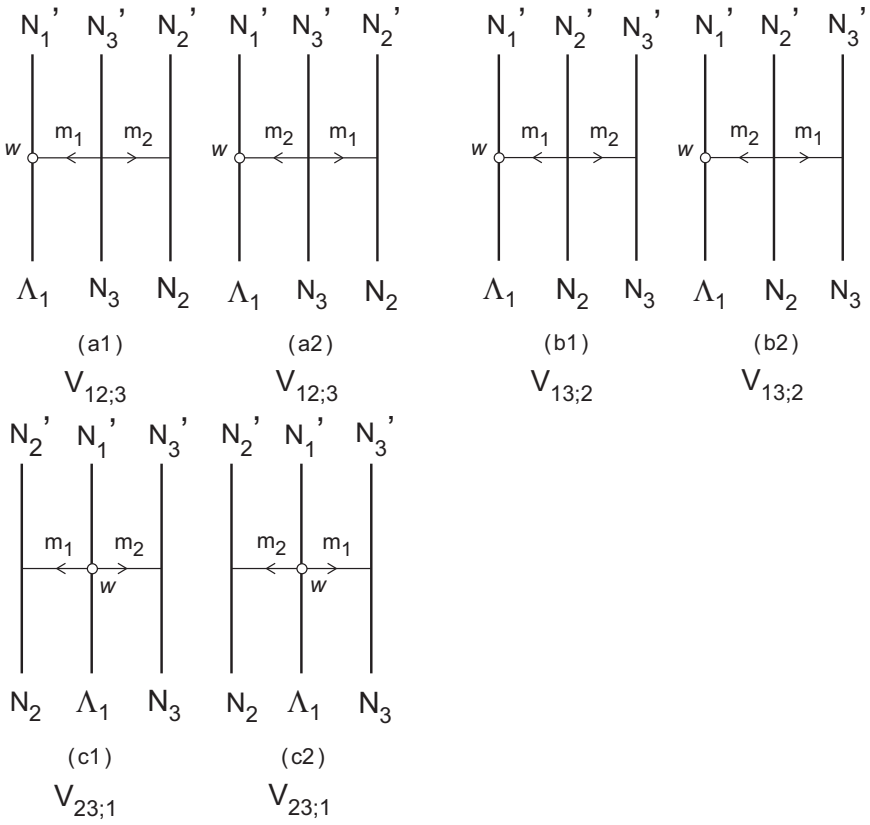

Fig. 1. Meson-pair exchange Feynman diagrams (a1)–(a2) of $V_{12;\,3}$, (b1)–(b2) of $V_{13;\,2}$, and (c1)–(c2) of $V_{23;\,1}$. $m1$ and $m2$ denote mesons. The open circle (○) represents a weak vertex. The pair of mesons $(m_1 m_2)$ represents $(\pi\pi)$, $(\pi\eta)$, $(\pi\rho)$, $(\pi\sigma)$, $(\pi\omega)$, or $(\sigma\sigma)$. In the case of $(\pi\pi)$ or $(\sigma\sigma)$ exchange, $m_1 = m_2 = \pi$ or $m_1 = m_2 = \sigma$, respectively.

two-body weak potentials starting with three-body associated diagrams. Next, in Sect. 4, the weak coupling constants are evaluated in the weak Λ–n mixing model by Dalitz–Von Hippel. In Sects. 5 and 6, we apply effective two-body weak potentials to evaluate the non-mesonic decay rates of the typical three hypernuclei and discuss the numerical results in comparison with the experimental data. Problems and limitations in the present treatment of the effective two-body potentials are also discussed in Sects. 5 and 6. A brief summary and some remarks on the present study are given in Sect. 7. In Appendix A, weak effective two-body interactions in momentum space for the meson-pair exchanges concerned are given.

2. Three-body weak $\Lambda NN \to NNN$ interactions in the meson-pair exchange model

We first construct the strangeness-changing ($\Delta S = 1$) three-body weak $\Lambda NN \to NNN$ interactions that cause the two-nucleon induced non-mesonic weak decays of hypernuclei.

One of the authors (Th.A.R.) introduced the idea of meson-pair exchange between baryons in the strong process early in the Nijmegen soft-core model [20] and also in the ESC model in various versions [21–27].

Following the ESC model [21–27] and the GESC model [28], the exchanged meson pairs adopted here consist of the following six categories:

(i) $J^{PC} = 0^{++}$: $(\pi\pi)_0$, $(\pi\eta)$, $(\sigma\sigma)$
(ii) $J^{PC} = 1^{--}$: $(\pi\pi)_1$

(iii) $J^{PC} = 1^{++}$: $(\pi\rho)_1$, $(\pi\sigma)$
(iv) $J^{PC} = 1^{+-}$: $(\pi\omega)$
(v) $J^P = 0^+$: $(K\pi)$
(vi) Fujita–Miyazawa $(\pi\pi)$

The strong NN(meson-pair) and $\Lambda N(K\pi)$ coupling interaction Hamiltonians are expressed in the standard way as follows:

$$J^{PC} = 0^{++} \ : \ \mathcal{H}_{NN(\pi\pi)_0} = g_{(\pi\pi)_0}[\bar{\psi}_N \psi_N](\boldsymbol{\varphi}_\pi \cdot \boldsymbol{\varphi}_\pi)/m_\pi \tag{1}$$

$$\mathcal{H}_{NN(\pi\eta)} = g_{(\pi\eta)}[\bar{\psi}_N \boldsymbol{\tau} \psi_N] \cdot \boldsymbol{\varphi}_\pi \phi_\eta / m_\pi \tag{2}$$

$$\mathcal{H}_{NN(\sigma\sigma)} = g_{(\sigma\sigma)}[\bar{\psi}_N \psi_N](\phi_\sigma)^2/m_\pi \tag{3}$$

$$\begin{aligned} J^{PC} = 1^{--} \ : \ \mathcal{H}_{NN(\pi\pi)_1} &= g_{(\pi\pi)_1}[\bar{\psi}_N \gamma_\mu \boldsymbol{\tau} \psi_N] \cdot (\boldsymbol{\varphi}_\pi \times \partial^\mu \boldsymbol{\varphi}_\pi)/m_\pi^2 \\ &- \frac{f_{(\pi\pi)_1}}{2M}[\bar{\psi}_N \sigma_{\mu\nu} \boldsymbol{\tau} \psi_N] \cdot \partial^\nu (\boldsymbol{\varphi}_\pi \times \partial^\mu \boldsymbol{\varphi}_\pi)/m_\pi^2 \end{aligned} \tag{4}$$

$$J^{PC} = 1^{++} \ : \ \mathcal{H}_{NN(\pi\rho)_1} = g_{(\pi\rho)_1}[\bar{\psi}_N \gamma_\mu \gamma_5 \boldsymbol{\tau} \psi_N] \cdot (\boldsymbol{\varphi}_\pi \times \boldsymbol{\phi}_\rho^\mu)/m_\pi \tag{5}$$

$$\mathcal{H}_{NN(\pi\sigma)} = g_{(\pi\sigma)}[\bar{\psi}_N \gamma_\mu \gamma_5 \boldsymbol{\tau} \psi_N] \cdot (\boldsymbol{\varphi}_\pi \partial^\mu \phi_\sigma - \phi_\sigma \partial^\mu \boldsymbol{\varphi}_\pi)/m_\pi^2 \tag{6}$$

$$J^{PC} = 1^{+-} \ : \ \mathcal{H}_{NN(\pi\omega)} = i\, g_{(\pi\omega)}[\bar{\psi}_N \sigma_{\mu\nu} \gamma_5 \boldsymbol{\tau} \psi_N] \cdot \partial^\nu (\boldsymbol{\varphi}_\pi \phi_\omega^\mu)/m_\pi^2 \tag{7}$$

$$J^P \ = \ 0^+ \ : \ \mathcal{H}_{\Lambda N(K\pi)} = g_{(K\pi)}[\bar{\psi}_N \boldsymbol{\tau} \phi^K] \cdot \boldsymbol{\varphi}_\pi \psi_\Lambda / m_\pi \tag{8}$$

$$\begin{aligned} \text{Fujita-Miyazawa} \ : \ \mathcal{H}_{FM(\pi\pi)} = -\bar{\psi}_N \Bigg[\Bigg\{ \Bigg((A+B)\frac{1}{m_\pi^3} \boldsymbol{\nabla}_1 \cdot \boldsymbol{\nabla}_2 + D \frac{1}{m_\pi} \Bigg) \delta_{ij} \\ - \ (A-B)\frac{1}{m_\pi^3} \boldsymbol{\sigma} \cdot (\boldsymbol{\nabla}_1 \times \boldsymbol{\nabla}_2) \epsilon_{ijk} \tau_k \Bigg\} \varphi_{\pi 1,i}(x)\, \varphi_{\pi 2,j}(x) \Bigg] \psi_N. \end{aligned} \tag{9}$$

The Fujita–Miyazawa $\mathcal{H}_{FM(\pi\pi)}$ is unique in the sense that it contains the effect of the Δ_{33} isobar in the vertex through the coupling constants [19].

Corresponding to the strong Hamiltonians shown above, the weak ΛN(meson-pair) and $NN(K\pi)$ coupling interaction Hamiltonians are expressed as follows, where the $\Delta I = 1/2$ rule is assumed.

$$J^{PC} = 0^{++} \ : \ \mathcal{H}^w_{\Lambda N(\pi\pi)_0} = G_F\, m_\pi^2 \left[\bar{\psi}_N \left(A^{pc}_{(\pi\pi)_0} + B^{pv}_{(\pi\pi)_0} \gamma_5 \right) \binom{0}{1} \psi_\Lambda \right] (\boldsymbol{\varphi}_\pi \cdot \boldsymbol{\varphi}_\pi)/m_\pi \tag{10}$$

$$\mathcal{H}^w_{\Lambda N(\pi\eta)} = G_F\, m_\pi^2 \left[\bar{\psi}_N \left(A^{pc}_{(\pi\eta)} + B^{pv}_{(\pi\eta)} \gamma_5 \right) \boldsymbol{\tau} \binom{0}{1} \psi_\Lambda \right] \cdot \boldsymbol{\varphi}_\pi \phi_\eta / m_\pi \tag{11}$$

$$\mathcal{H}^w_{\Lambda N(\sigma\sigma)} = G_F\, m_\pi^2 \left[\bar{\psi}_N \left(A^{pc}_{(\sigma\sigma)} + B^{pv}_{(\sigma\sigma)} \gamma_5 \right) \binom{0}{1} \psi_\Lambda \right] (\phi_\sigma)^2/m_\pi \tag{12}$$

$$J^{PC}=1^{--}\ :\ \mathcal{H}^{w}_{\Lambda N(\pi\pi)_1}=G_F\,m_\pi^2\left[\bar\psi_N\Big\{\alpha_{(\pi\pi)_1}\gamma_\mu-i\,\beta_{(\pi\pi)_1}\frac{\sigma_{\mu\nu}(p_\Lambda-p_N)^\nu}{2M}+\varepsilon_{(\pi\pi)_1}\gamma_\mu\gamma_5\Big\}\boldsymbol{\tau}\binom{0}{1}\psi_\Lambda\right]\cdot(\boldsymbol{\varphi}_\pi\times\partial^\mu\boldsymbol{\varphi}_\pi)/m_\pi^2 \tag{13}$$

$$J^{PC}=1^{++}\ :\ \mathcal{H}^{w}_{\Lambda N(\pi\rho)_1}=G_F\,m_\pi^2\left[\bar\psi_N\left\{A^{pc}_{(\pi\rho)_1}\gamma_\mu\gamma_5+B^{pv}_{(\pi\rho)_1}\gamma_\mu\right\}\boldsymbol{\tau}\binom{0}{1}\psi_\Lambda\right]\cdot(\boldsymbol{\varphi}_\pi\times\boldsymbol{\phi}^\mu_\rho)/m_\pi \tag{14}$$

$$\mathcal{H}^{w}_{\Lambda N(\pi\sigma)}=G_F\,m_\pi^2\left[\bar\psi_N\left\{A^{pc}_{(\pi\sigma)}\gamma_\mu\gamma_5+B^{pv}_{(\pi\sigma)}\gamma_\mu\right\}\boldsymbol{\tau}\binom{0}{1}\psi_\Lambda\right]\cdot(\boldsymbol{\varphi}_\pi\partial^\mu\phi_\sigma-\phi_\sigma\partial^\mu\boldsymbol{\varphi}_\pi)/m_\pi^2 \tag{15}$$

$$J^{PC}=1^{+-}\ :\ \mathcal{H}^{w}_{\Lambda N(\pi\omega)}=i\,G_F\,m_\pi^2\left[\bar\psi_N\left\{A^{pc}_{(\pi\omega)}\sigma_{\mu\nu}\gamma_5+B^{pv}_{(\pi\omega)}\sigma_{\mu\nu}\right\}\boldsymbol{\tau}\binom{0}{1}\psi_\Lambda\right]\cdot\partial^\nu(\boldsymbol{\varphi}_\pi\phi^\mu_\omega)/m_\pi^2 \tag{16}$$

$$J^{P}=0^{+}\ :\ \mathcal{H}^{w}_{NN(K\pi)}=G_F\,m_\pi^2\left[[\bar\psi_N\binom{0}{1}\left(C^{pc}_{(K\pi)}+C^{pv}_{(K\pi)}\gamma_5\right)(\phi^K)^\dagger\boldsymbol{\tau}\psi_N\cdot\boldsymbol{\varphi}_\pi+\bar\psi_N\left(D^{pc}_{(K\pi)}+D^{pv}_{(K\pi)}\gamma_5\right)\boldsymbol{\tau}\psi_N\cdot\boldsymbol{\varphi}_\pi(\phi^K)^\dagger\binom{0}{1}\right]/m_\pi. \tag{17}$$

The nucleon field ψ_N and the kaon field ϕ^K represent the isospin doublets as

$$\psi_N=\begin{pmatrix}\psi_p\\ \psi_n\end{pmatrix}\ \text{ and }\ \phi^K=\begin{pmatrix}\phi^{K^+}\\ \phi^{K^0}\end{pmatrix}, \tag{18}$$

respectively. In Eqs. (10)–(17), the isospin spurion $\binom{0}{1}$ is used to enforce that the weak Hamiltonians should follow the $\Delta I=1/2$ rule.

It is noted that we omit the weak Fujita–Miyazawa-type $(\pi\pi)$-pair coupling Hamiltonian because we do not know it now.

The strong and weak interaction Hamiltonians for the baryon–baryon–meson coupling are given in Ref. [6].

Figure 1 shows the Feynman diagrams for the (m_1m_2)-meson-pair exchange weak $\Lambda NN\to NNN$ transition interaction. The (m_1m_2) pair represents one of the pairs $(\pi\pi)$, $(\pi\eta)$, $(\pi\rho)$, $(\pi\sigma)$, $(\pi\omega)$, or $(\sigma\sigma)$. For the Fujita–Miyazawa $(\pi\pi)$ exchange, the diagrams are the same as those for the $(\pi\pi)$ exchange except for the interpretation of meson-pair vertices. Note that the $(K\pi)$-pair exchange Feynman diagrams for the weak $\Lambda NN\to NNN$ interaction are not included in Fig. 1, since the NNK- and/or $NN(K\pi)$-vertex in the diagrams represent the weak ones in the $(K\pi)$-pair exchange case. The Feynman diagrams depicted in Fig. 1 can be evaluated in momentum space, once the momenta are assigned as $(\boldsymbol{p}_{1\boldsymbol{\Lambda}},\boldsymbol{p}_2,\boldsymbol{p}_3)$ for (Λ_1,N_2,N_3) and $(\boldsymbol{p}'_1,\boldsymbol{p}'_2,\boldsymbol{p}'_3)$ for (N'_1,N'_2,N'_3), respectively. We note that the Λ hyperon is assigned as particle 1, and keep this hereafter in this paper.

In the case of $(\pi\sigma)$ exchange, for Fig. 1(a1) we obtain $(V^{(\mathrm{a1})}_{12;3})_{(\pi\sigma)}(\boldsymbol{p}'_1,\boldsymbol{p}'_2,\boldsymbol{p}'_3,\boldsymbol{p}_{1\boldsymbol{\Lambda}},\boldsymbol{p}_2,\boldsymbol{p}_3)$, and similarly for Fig. 1(a2) $(V^{(\mathrm{a2})}_{12;3})_{(\pi\sigma)}(\boldsymbol{p}'_1,\boldsymbol{p}'_2,\boldsymbol{p}'_3,\boldsymbol{p}_{1\boldsymbol{\Lambda}},\boldsymbol{p}_2,\boldsymbol{p}_3)$. By adding these two terms, we get

$$\left(V^{(\mathrm{a})}_{12;3}\right)_{(\pi\sigma)}=\left(V^{(\mathrm{a1})}_{12;3}\right)_{(\pi\sigma)}+\left(V^{(\mathrm{a2})}_{12;3}\right)_{(\pi\sigma)}. \tag{19}$$

The complete three-body MPE interaction of $(\pi\sigma)$ exchange is obtained by the sum over the three types of permutations as

$$V^{\mathrm{W3B}}_{(\pi\sigma)} = \left(V^{(\mathrm{a})}_{12;3}\right)_{(\pi\sigma)} + \left(V^{(\mathrm{b})}_{13;2}\right)_{(\pi\sigma)} + \left(V^{(\mathrm{c})}_{23;1}\right)_{(\pi\sigma)}. \tag{20}$$

Now we rearrange the r.h.s. of Eq. (20) for convenience of expression in the following as

$$V^{\mathrm{W3B}}_{(\pi\sigma)} = V^{(1)}_{(\pi\sigma)} + V^{(2)}_{(\pi\sigma)} + V^{(3)}_{(\pi\sigma)}, \tag{21}$$

where

$$V^{(1)}_{(\pi\sigma)} = V^{(\mathrm{a1})}_{(\pi\sigma)} + V^{(\mathrm{b1})}_{(\pi\sigma)}, \quad V^{(2)}_{(\pi\sigma)} = V^{(\mathrm{a2})}_{(\pi\sigma)} + V^{(\mathrm{b2})}_{(\pi\sigma)}, \quad V^{(3)}_{(\pi\sigma)} = V^{(\mathrm{c1})}_{(\pi\sigma)} + V^{(\mathrm{c2})}_{(\pi\sigma)}. \tag{22}$$

Introducing a new set of variables

$$\boldsymbol{q}_i = \frac{1}{2}\left(\boldsymbol{p}_i + \boldsymbol{p}'_i\right), \quad \boldsymbol{k}_i = \boldsymbol{p}'_i - \boldsymbol{p}_i, \tag{23}$$

the terms on the r.h.s. of Eq. (21) are expressed in the leading terms and the next higher-order terms in $(\boldsymbol{p}^2/M^2)$ when the Feynman diagram is evaluated in the momentum space as follows:

$$\begin{aligned}
V^{(1)}_{(\pi\sigma)} = \frac{g_{(\pi\sigma)}}{m_\pi^2} g^w_\pi g_\sigma 2M_N \times \Bigg[& \left\{ \lambda \frac{(\boldsymbol{\sigma}_1\cdot\boldsymbol{k}_1)}{2\bar{M}} \left[\frac{\boldsymbol{\sigma}_3\cdot(\boldsymbol{k}_1-\boldsymbol{k}_2)}{2M_N} - \frac{\boldsymbol{\sigma}_3\cdot\boldsymbol{q}_3}{M_N}\left(\frac{\boldsymbol{q}_1\cdot\boldsymbol{k}_1}{2\bar{M}M_N} - \frac{\boldsymbol{q}_2\cdot\boldsymbol{k}_2}{2{M_N}^2}\right)\right.\right. \\
& \left.\left. + \frac{\boldsymbol{\sigma}_3\cdot(\boldsymbol{k}_1-\boldsymbol{k}_2)}{2M_N}\left(\frac{\boldsymbol{k}_2^2}{8{M_N}^2} - \frac{i\boldsymbol{\sigma}_2\cdot(\boldsymbol{k}_2\times\boldsymbol{q}_2)}{4{M_N}^2}\right)\right] \right. \\
& - \left[\frac{\boldsymbol{\sigma}_3\cdot(\boldsymbol{k}_1-\boldsymbol{k}_2)}{2M_N} - \frac{\boldsymbol{\sigma}_3\cdot\boldsymbol{q}_3}{M_N}\left(\frac{\boldsymbol{q}_1\cdot\boldsymbol{k}_1}{2\bar{M}M_N} - \frac{\boldsymbol{q}_2\cdot\boldsymbol{k}_2}{2{M_N}^2}\right)\right. \\
& + \frac{\boldsymbol{\sigma}_3\cdot(\boldsymbol{k}_1-\boldsymbol{k}_2)}{2M_N}\left(\frac{\boldsymbol{k}_1^2}{8\bar{M}^2} + \frac{\boldsymbol{k}_2^2}{8{M_N}^2}\right. \\
& \left.\left.\left. - \frac{i\boldsymbol{\sigma}_1\cdot(\boldsymbol{k}_1\times\boldsymbol{q}_1)}{4\bar{M}^2} - \frac{i\boldsymbol{\sigma}_2\cdot(\boldsymbol{k}_2\times\boldsymbol{q}_2)}{4{M_N}^2}\right)\right] \right\} \frac{1}{\boldsymbol{k}_1^2+m_\pi^2}\frac{1}{\boldsymbol{k}_2^2+m_\sigma^2}(\boldsymbol{\tau}_3\cdot\boldsymbol{\tau}_1) \\
& + \left\{ \lambda \frac{(\boldsymbol{\sigma}_1\cdot\boldsymbol{k}_1)}{2\bar{M}} \left[\frac{\boldsymbol{\sigma}_2\cdot(\boldsymbol{k}_1-\boldsymbol{k}_3)}{2M_N} - \frac{\boldsymbol{\sigma}_2\cdot\boldsymbol{q}_2}{M_N}\left(\frac{\boldsymbol{q}_1\cdot\boldsymbol{k}_1}{2\bar{M}M_N} - \frac{\boldsymbol{q}_3\cdot\boldsymbol{k}_3}{2{M_N}^2}\right)\right.\right. \\
& \left.\left. + \frac{\boldsymbol{\sigma}_2\cdot(\boldsymbol{k}_1-\boldsymbol{k}_3)}{2M_N}\left(\frac{\boldsymbol{k}_3^2}{8{M_N}^2} - \frac{i\boldsymbol{\sigma}_3\cdot(\boldsymbol{k}_3\times\boldsymbol{q}_3)}{4{M_N}^2}\right)\right] \right. \\
& - \left[\frac{\boldsymbol{\sigma}_2\cdot(\boldsymbol{k}_1-\boldsymbol{k}_3)}{2M_N} - \frac{\boldsymbol{\sigma}_2\cdot\boldsymbol{q}_2}{M_N}\left(\frac{\boldsymbol{q}_1\cdot\boldsymbol{k}_1}{2\bar{M}M_N} - \frac{\boldsymbol{q}_3\cdot\boldsymbol{k}_3}{2{M_N}^2}\right)\right. \\
& + \frac{\boldsymbol{\sigma}_2\cdot(\boldsymbol{k}_1-\boldsymbol{k}_3)}{2M_N}\left(\frac{\boldsymbol{k}_1^2}{8\bar{M}^2} + \frac{\boldsymbol{k}_3^2}{8{M_N}^2}\right. \\
& \left.\left.\left. - \frac{i\boldsymbol{\sigma}_1\cdot(\boldsymbol{k}_1\times\boldsymbol{q}_1)}{4\bar{M}^2} - \frac{i\boldsymbol{\sigma}_3\cdot(\boldsymbol{k}_3\times\boldsymbol{q}_3)}{4{M_N}^2}\right)\right] \right\} \cdot \frac{1}{\boldsymbol{k}_1^2+m_\pi^2}\frac{1}{\boldsymbol{k}_3^2+m_\sigma^2}(\boldsymbol{\tau}_2\cdot\boldsymbol{\tau}_1) \Bigg],
\end{aligned} \tag{24}$$

$$
\begin{aligned}
V^{(2)}_{(\pi\sigma)} = &-\frac{g_{(\pi\sigma)}}{m_\pi^2} {G_F m_\pi}^2 \frac{f_\pi}{m_\pi} (2M_N)^2 \times \Bigg[\Bigg\{ A^{pc}_\sigma \frac{(\boldsymbol{\sigma}_2 \cdot \boldsymbol{k}_2)}{2M_N} \Bigg[\frac{\boldsymbol{\sigma}_3 \cdot (\boldsymbol{k}_1 - \boldsymbol{k}_2)}{2M_N} \\
&- \frac{\boldsymbol{\sigma}_3 \cdot \boldsymbol{q}_3}{M_N} \left(\frac{\boldsymbol{q}_1 \cdot \boldsymbol{k}_1}{2\bar{M} M_N} - \frac{\boldsymbol{q}_2 \cdot \boldsymbol{k}_2}{2{M_N}^2} \right) + \frac{\boldsymbol{\sigma}_3 \cdot (\boldsymbol{k}_1 - \boldsymbol{k}_2)}{2M_N} \left(\frac{\boldsymbol{k}_1^2}{8\bar{M}^2} - \frac{i\boldsymbol{\sigma}_1 \cdot (\boldsymbol{k}_1 \times \boldsymbol{q}_1)}{4\bar{M}^2} \right) \Bigg] \\
&- B^{pv}_\sigma \frac{(\boldsymbol{\sigma}_1 \cdot \boldsymbol{k}_1)}{2\bar{M}} \frac{(\boldsymbol{\sigma}_2 \cdot \boldsymbol{k}_2)}{2M_N} \frac{(\boldsymbol{\sigma}_3 \cdot (\boldsymbol{k}_1 - \boldsymbol{k}_2))}{2M_N} \Bigg\} \frac{1}{\boldsymbol{k}_1^2 + m_\sigma^2} \frac{1}{\boldsymbol{k}_2^2 + m_\pi^2} (\boldsymbol{\tau}_3 \cdot \boldsymbol{\tau}_2) \\
&+ \Bigg\{ A^{pc}_\sigma \frac{(\boldsymbol{\sigma}_3 \cdot \boldsymbol{k}_3)}{2M_N} \Bigg[\frac{\boldsymbol{\sigma}_2 \cdot (\boldsymbol{k}_1 - \boldsymbol{k}_3)}{2M_N} - \frac{\boldsymbol{\sigma}_2 \cdot \boldsymbol{q}_2}{M_N} \left(\frac{\boldsymbol{q}_1 \cdot \boldsymbol{k}_1}{2\bar{M} M_N} - \frac{\boldsymbol{q}_3 \cdot \boldsymbol{k}_3}{2{M_N}^2} \right) \\
&+ \frac{\boldsymbol{\sigma}_2 \cdot (\boldsymbol{k}_1 - \boldsymbol{k}_3)}{2M_N} \left(\frac{\boldsymbol{k}_1^2}{8\bar{M}^2} - \frac{i\boldsymbol{\sigma}_1 \cdot (\boldsymbol{k}_1 \times \boldsymbol{q}_1)}{4\bar{M}^2} \right) \Bigg] \\
&- B^{pv}_\sigma \frac{(\boldsymbol{\sigma}_1 \cdot \boldsymbol{k}_1)}{2\bar{M}} \frac{(\boldsymbol{\sigma}_3 \cdot \boldsymbol{k}_3)}{2M_N} \frac{(\boldsymbol{\sigma}_2 \cdot (\boldsymbol{k}_1 - \boldsymbol{k}_3))}{2M_N} \Bigg\} \frac{1}{\boldsymbol{k}_1^2 + m_\sigma^2} \frac{1}{\boldsymbol{k}_3^2 + m_\pi^2} (\boldsymbol{\tau}_2 \cdot \boldsymbol{\tau}_3) \Bigg], \qquad (25)
\end{aligned}
$$

$$
\begin{aligned}
V^{(3)}_{(\pi\sigma)} = &\frac{{G_F m_\pi}^2}{m_\pi^2} \frac{f_\pi}{m_\pi} g_\sigma (2M_N)^2 \times \Bigg[\Bigg\{ A^{pc}_{(\pi\sigma)} \frac{(\boldsymbol{\sigma}_2 \cdot \boldsymbol{k}_2)}{2M_N} \Bigg[\frac{\boldsymbol{\sigma}_1 \cdot (\boldsymbol{k}_2 - \boldsymbol{k}_3)}{2M_N} - \frac{\boldsymbol{\sigma}_1 \cdot \boldsymbol{q}_1}{\bar{M}} \left(\frac{\boldsymbol{q}_2 \cdot \boldsymbol{k}_2}{2{M_N}^2} - \frac{\boldsymbol{q}_3 \cdot \boldsymbol{k}_3}{2{M_N}^2} \right) \\
&+ \frac{\boldsymbol{\sigma}_1 \cdot (\boldsymbol{k}_2 - \boldsymbol{k}_3)}{2M_N} \left(\frac{\boldsymbol{k}_3^2}{8{M_N}^2} - \frac{i\boldsymbol{\sigma}_3 \cdot (\boldsymbol{k}_3 \times \boldsymbol{q}_3)}{4{M_N}^2} \right) \Bigg] \\
&+ B^{pv}_{(\pi\sigma)} \frac{(\boldsymbol{\sigma}_2 \cdot \boldsymbol{k}_2)}{2M_N} \Bigg[\frac{\boldsymbol{q}_1 \cdot (\boldsymbol{k}_2 - \boldsymbol{k}_3)}{2\bar{M} M_N} - \frac{\boldsymbol{q}_2 \cdot \boldsymbol{k}_2 - \boldsymbol{q}_3 \cdot \boldsymbol{k}_3}{2M_N^2} \\
&+ \frac{i(\boldsymbol{\sigma}_1 \times \boldsymbol{k}_1) \cdot (\boldsymbol{k}_2 - \boldsymbol{k}_3)}{4\bar{M} M_N} \Bigg] \Bigg\} \frac{1}{\boldsymbol{k}_2^2 + m_\pi^2} \frac{1}{\boldsymbol{k}_3^2 + m_\sigma^2} (\boldsymbol{\tau}_1 \cdot \boldsymbol{\tau}_2) \\
&+ \Bigg\{ A^{pc}_{(\pi\sigma)} \frac{(\boldsymbol{\sigma}_3 \cdot \boldsymbol{k}_3)}{2M_N} \Bigg[\frac{\boldsymbol{\sigma}_1 \cdot (\boldsymbol{k}_3 - \boldsymbol{k}_2)}{2M_N} - \frac{\boldsymbol{\sigma}_1 \cdot \boldsymbol{q}_1}{\bar{M}} \left(\frac{\boldsymbol{q}_3 \cdot \boldsymbol{k}_3}{2{M_N}^2} - \frac{\boldsymbol{q}_2 \cdot \boldsymbol{k}_2}{2{M_N}^2} \right) \\
&+ \frac{\boldsymbol{\sigma}_1 \cdot (\boldsymbol{k}_3 - \boldsymbol{k}_2)}{2M_N} \left(\frac{\boldsymbol{k}_2^2}{8{M_N}^2} - \frac{i\boldsymbol{\sigma}_2 \cdot (\boldsymbol{k}_2 \times \boldsymbol{q}_2)}{4{M_N}^2} \right) \Bigg] \\
&+ B^{pv}_{(\pi\sigma)} \frac{(\boldsymbol{\sigma}_3 \cdot \boldsymbol{k}_3)}{2M_N} \Bigg[\frac{\boldsymbol{q}_1 \cdot (\boldsymbol{k}_3 - \boldsymbol{k}_2)}{2\bar{M} M_N} - \frac{\boldsymbol{q}_3 \cdot \boldsymbol{k}_3 - \boldsymbol{q}_2 \cdot \boldsymbol{k}_2}{2M_N^2} \\
&+ \frac{i(\boldsymbol{\sigma}_1 \times \boldsymbol{k}_1) \cdot (\boldsymbol{k}_3 - \boldsymbol{k}_2)}{4\bar{M} M_N} \Bigg] \Bigg\} \frac{1}{\boldsymbol{k}_3^2 + m_\pi^2} \frac{1}{\boldsymbol{k}_2^2 + m_\sigma^2} (\boldsymbol{\tau}_1 \cdot \boldsymbol{\tau}_3) \Bigg]. \qquad (26)
\end{aligned}
$$

Likewise the expressions of the three-body interaction for meson-pair exchanges other than $(\pi\sigma)$ exchange can be written down easily.

The three-body interaction in the configuration space is given by the Fourier transform of that in the momentum space of $V^{\mathrm{W3B}}(\boldsymbol{p}'_1, \boldsymbol{p}'_2, \boldsymbol{p}'_3;\ \boldsymbol{p}_1, \boldsymbol{p}_2, \boldsymbol{p}_3) \equiv V^{\mathrm{W3B}}(\boldsymbol{k}_1, \boldsymbol{k}_2, \boldsymbol{k}_3;\ \boldsymbol{q}_1, \boldsymbol{q}_2, \boldsymbol{q}_3)$. If the interaction depends only on the $\boldsymbol{k}_i$ variables, one obtains

$$V^{\mathrm{W3B}}(\boldsymbol{x}_1', \boldsymbol{x}_2', \boldsymbol{x}_3';\ \boldsymbol{x}_1, \boldsymbol{x}_2, \boldsymbol{x}_3) = \delta(\boldsymbol{x}_1' - \boldsymbol{x}_1)\delta(\boldsymbol{x}_2' - \boldsymbol{x}_2)\delta(\boldsymbol{x}_3' - \boldsymbol{x}_3)$$
$$\times \prod_{i=1,3}\left[\int \frac{d^3\boldsymbol{k}_i}{(2\pi)^3} e^{i\boldsymbol{k}_i\cdot\boldsymbol{x}_i}\right](2\pi)^3\delta(\boldsymbol{k}_1 + \boldsymbol{k}_2 + \boldsymbol{k}_3)$$
$$\times V^{\mathrm{W3B}}(\boldsymbol{k}_1, \boldsymbol{k}_2, \boldsymbol{k}_3) \tag{27}$$
$$= \delta(\boldsymbol{x}_1' - \boldsymbol{x}_1)\delta(\boldsymbol{x}_2' - \boldsymbol{x}_2)\delta(\boldsymbol{x}_3' - \boldsymbol{x}_3)$$
$$\times \int \frac{d^3\boldsymbol{k}_1}{(2\pi)^3}\int \frac{d^3\boldsymbol{k}_2}{(2\pi)^3} e^{i\boldsymbol{k}_1\cdot(\boldsymbol{x}_1 - \boldsymbol{x}_3)} e^{i\boldsymbol{k}_2\cdot(\boldsymbol{x}_2 - \boldsymbol{x}_3)}$$
$$\times V^{\mathrm{W3B}}(\boldsymbol{k}_1, \boldsymbol{k}_2). \tag{28}$$

If the interaction has $\boldsymbol{q}_i$-dependence in $V^{\mathrm{W3B}}(\boldsymbol{k}_1, \boldsymbol{k}_2, \boldsymbol{k}_3;\ \boldsymbol{q}_1, \boldsymbol{q}_2, \boldsymbol{q}_3)$, we need to handle the interaction in an approximation in which the non-local operator with $\boldsymbol{q}_i$-dependence is replaced by the operator with no $\boldsymbol{q}_i$-dependence. In this paper the prescription will be explained in Sect. 3.2.

3. Effective two-body $\Lambda N \to NN$ potentials

3.1 *Kinematical restrictions and the effective two-body potential*

The effective two-body potential can be derived by integrating out the degrees of freedom (space, spin, and isospin) of, say, a nucleon "3", following the Loiseau–Nogami–Ross (LNR) approximation method [29]. The kinematical restrictions and momentum conservations should be noted. The momentum conservation holds in the three-particle system:

$$\boldsymbol{p}_{1\Lambda} + \boldsymbol{p}_2 + \boldsymbol{p}_3 = \boldsymbol{p}_1' + \boldsymbol{p}_2' + \boldsymbol{p}_3'. \tag{29}$$

In the effective two-body potential, we must require momentum conservation, i.e.,

$$\boldsymbol{P} = \boldsymbol{p}_{1\Lambda} + \boldsymbol{p}_2 = \boldsymbol{p}_1' + \boldsymbol{p}_2' = \boldsymbol{P}'. \tag{30}$$

Further we are going to work in the two-particle CM-system as

$$\boldsymbol{P} = 0 \quad \text{and} \quad \boldsymbol{p}_3' = \boldsymbol{p}_3. \tag{31}$$

This implies

$$\boldsymbol{q}_2 = -\boldsymbol{q}_1, \quad \boldsymbol{k}_2 = -\boldsymbol{k}_1, \quad \text{and} \quad \boldsymbol{k}_3 = 0. \tag{32}$$

Thus one sees straightforwardly

$$V^{W3B}(\boldsymbol{k}_1, \boldsymbol{k}_2, \boldsymbol{k}_3;\ \boldsymbol{q}_1, \boldsymbol{q}_2, \boldsymbol{q}_3) \longrightarrow V^{W3B}(\boldsymbol{k}_1, -\boldsymbol{k}_1, 0\ ;\ \boldsymbol{q}_1, -\boldsymbol{q}_1, \boldsymbol{q}_3). \tag{33}$$

In nuclear matter, one averages over $\boldsymbol{p}_3 = \boldsymbol{q}_3$ [30]. This means that only the quadratic term survives, i.e., $< \boldsymbol{q}_3^2 >= (3/5)k_F^2$ and $< \boldsymbol{q}_3 >= 0$.

Now in the case that the three-body interaction has no $\boldsymbol{q}_i$-dependence or it is treated as having no $\boldsymbol{q}_i$-dependence in the prescription of the local operator approximation for the non-local

operator, we have the effective two-body $\Lambda N \to NN$ potential as

$$
\begin{aligned}
V^{(\mathrm{eff.2B})}(1,2) &= \frac{1}{4}\rho_{NM}\,Tr\int d^3\boldsymbol{x}_3 V^{\mathrm{W3B}}(\boldsymbol{x}_1,\boldsymbol{x}_2,\boldsymbol{x}_3) \\
&= \frac{1}{4}\rho_{NM}\,Tr\int d^3\boldsymbol{x}_3\int\frac{d^3\boldsymbol{k}_1}{(2\pi)^3}\int\frac{d^3\boldsymbol{k}_2}{(2\pi)^3}e^{i\boldsymbol{k}_1\cdot(\boldsymbol{x}_1-\boldsymbol{x}_3)}e^{i\boldsymbol{k}_2\cdot(\boldsymbol{x}_2-\boldsymbol{x}_3)} \\
&\quad\times V^{\mathrm{W3B}}(\boldsymbol{k}_1,\boldsymbol{k}_2)\big|_{\boldsymbol{k}_3=-\boldsymbol{k}_1-\boldsymbol{k}_2} \\
&= \frac{1}{4}\rho_{NM}\,Tr\int\frac{d^3\boldsymbol{k}}{(2\pi)^3}e^{i\boldsymbol{k}\cdot(\boldsymbol{x}_1-\boldsymbol{x}_2)}V^{\mathrm{W3B}}(\boldsymbol{k},-\boldsymbol{k}), \\
&= \rho_{NM}\int\frac{d^3\boldsymbol{k}}{(2\pi)^3}e^{i\boldsymbol{k}\cdot(\boldsymbol{x}_1-\boldsymbol{x}_2)}\tilde{V}^{W}(\boldsymbol{k},-\boldsymbol{k}),
\end{aligned}
\tag{34}
$$

where $\rho_{NM} = 2{k_F}^3/3\pi^2$ (with $k_F = 1.4\,\mathrm{fm}^{-1}$) for symmetric nuclear matter. In Eq. (34) the *Tr*-symbol stands for trace over the spin and isospin operator of nucleon "3". The concrete expression of $\tilde{V}^{W}(\boldsymbol{k},-\boldsymbol{k})$ in Eq. (34) is actually obtained after the $\boldsymbol{q}$-operator in $\tilde{V}^{W}(\boldsymbol{k},-\boldsymbol{k},\boldsymbol{q})$ given in Appendix A is treated in the way described in the next subsection.

3.2 *LNR approximation and the local momentum approximation*

The LNR approximation applied in Eq. (34) acts to diminish some of the contributions derived from the weak three-body interactions considered for MPE (i)–(vi) in Sect. 2. For example, the $(\pi\pi)_1$-, $(\pi\eta)$-, and $(\pi\rho)_1$-exchange interactions vanish completely. This is because those weak three-body interactions contain $(\boldsymbol{\tau}_3\cdot(\boldsymbol{\tau}_1\times\boldsymbol{\tau}_2))$ and/or $(\boldsymbol{\tau}_3\cdot\boldsymbol{\tau}_1)$, $(\boldsymbol{\tau}_3\cdot\boldsymbol{\tau}_2)$, $(\boldsymbol{\sigma}_3\cdot\boldsymbol{k}_3)$, etc. and such operators vanish when the trace operators are applied to $\boldsymbol{\tau}_3$ and $\boldsymbol{\sigma}_3$. One also knows that some limited number of terms remain for the $(\pi\pi)_0$-, $(\pi\sigma)$-, $(\pi\omega)$-, $(K\pi)$-, $(\sigma\sigma)$-, and Fujita–Miyazawa $(\pi\pi)$-pair exchange effective two-body interactions after applying the *Tr*-operation; $Tr(\boldsymbol{\tau}_3) = Tr(\boldsymbol{\sigma}_3) = 0$ on $V^{\mathrm{W3B}}(\boldsymbol{k},-\boldsymbol{k})$.

The reduced effective two-body interactions $\tilde{V}^{W}(\boldsymbol{k},-\boldsymbol{k},\boldsymbol{q})$ for $(\pi\pi)_0$, $(\pi\sigma)$, $(\pi\omega)$, $(K\pi)$, $(\sigma\sigma)$, and Fujita–Miyazawa $(\pi\pi)$ exchanges in momentum space are given in Appendix A.

Here we notice that non-local operators of the form $(\boldsymbol{\sigma}_2\cdot\boldsymbol{q})(\boldsymbol{q}\cdot\boldsymbol{k})$ and $(\boldsymbol{q}\cdot\boldsymbol{k})(\boldsymbol{\sigma}_2\cdot\boldsymbol{k})$ exist in $\tilde{V}^{W}_{(\pi\sigma)}(\boldsymbol{k},-\boldsymbol{k},\,;\,\boldsymbol{q},)$ of the $(\pi\sigma)$ exchange. For the $(\boldsymbol{\sigma}_2\cdot\boldsymbol{q})(\boldsymbol{q}\cdot\boldsymbol{k})$-operator, we like to separate the non-local operator part and the local part of that operator as

$$
(\boldsymbol{q}\cdot\boldsymbol{k})(\boldsymbol{\sigma}_2\cdot\boldsymbol{q}) = \left[(\boldsymbol{q}\cdot\boldsymbol{k})(\boldsymbol{\sigma}_2\cdot\boldsymbol{q}) + \frac{1}{4}\boldsymbol{k}^2(\boldsymbol{\sigma}_2\cdot\boldsymbol{k})\right] - \frac{1}{4}\boldsymbol{k}^2(\boldsymbol{\sigma}_2\cdot\boldsymbol{k}),
\tag{35}
$$

in which the first term on the r.h.s. in Eq. (35) is a non-local operator and the second one is a local operator. That this separation is plausible is proved in Ref. [28]. We adopt the local operator part only, so that

$$
(\boldsymbol{\sigma}_1\cdot\boldsymbol{k})(\boldsymbol{\sigma}_2\cdot\boldsymbol{q})(\boldsymbol{q}\cdot\boldsymbol{k}) \approx -\frac{1}{4}\boldsymbol{k}^2(\boldsymbol{\sigma}_1\cdot\boldsymbol{k})(\boldsymbol{\sigma}_2\cdot\boldsymbol{k}).
\tag{36}
$$

This is the local operator approximation and we apply Eq. (36) to $\tilde{V}^{W}(\boldsymbol{k},-\boldsymbol{k},\boldsymbol{q})$. For the second operator $(\boldsymbol{q}\cdot\boldsymbol{k})(\boldsymbol{\sigma}_2\cdot\boldsymbol{k})$, we simply drop it.

The form factor is introduced for each meson propagator such that

$$
\frac{1}{\boldsymbol{k}^2+m^2} \to \frac{F(\boldsymbol{k}^2)}{\boldsymbol{k}^2+m^2},
\tag{37}
$$

and we take

$$
F\left(\boldsymbol{k}^2\right) = \exp\left(-\boldsymbol{k}^2/\Lambda_m^2\right),
\tag{38}
$$

which is a Gaussian form and Λ_m is a cut-off mass for the meson m. Note, however, that, in the case of the Fujita–Miyazawa $(\pi\pi)$-exchange interaction, we take the form factor as

$$F\left(\boldsymbol{k}^2\right) = \exp\left(-\boldsymbol{k}^2/\Lambda_F^2\right). \tag{39}$$

3.3 *Configuration space effective two-body $\Lambda N \to NN$ potentials*

The effective two-body $\Lambda N \to NN$ potentials in the configuration space are listed below following the prescriptions mentioned in the preceding subsections. The spin–orbit-like part of potentials is neglected in the configuration space for simplicity. We write $\boldsymbol{r} = \boldsymbol{x}_1 - \boldsymbol{x}_2$ in the following expressions.

1. $J^{PC} = 0^{++}$; $(\pi\pi)_0$-pair exchange

$$\begin{aligned}
V^{(\mathrm{eff.2B})}_{(\pi\pi)_0}(r) = {} & \frac{4\pi\,\rho_{NM}}{m_\pi^3}\frac{g_{(\pi\pi)_0}g_\pi^w}{4\pi}\frac{f_\pi}{4\pi}\frac{2M_N}{m_\pi}\,m_\pi \\
& \times\Bigg\{\lambda\ (\boldsymbol{\sigma}_1\cdot\boldsymbol{\sigma}_2)\,(\boldsymbol{\tau}_1\cdot\boldsymbol{\tau}_2)\ \frac{1}{3}\,\frac{m_\pi^2}{4\bar{M}M_N}\Bigg[\left(1+\frac{2m_\pi^2}{\Lambda_\pi^2}\right)\phi_C^0\left(m_\pi,\,\frac{\Lambda_\pi}{\sqrt{2}},\,r\right) \\
& -\frac{1}{4}\exp\left(2m_\pi^2/\Lambda_\pi^2\right)\Bigg\{e^{-m_\pi r}\mathrm{Erfc}\left(-\frac{\Lambda_\pi r}{2\sqrt{2}}+\frac{\sqrt{2}m_\pi}{\Lambda_\pi}\right) \\
& +e^{m_\pi r}\mathrm{Erfc}\left(\frac{\Lambda_\pi r}{2\sqrt{2}}+\frac{\sqrt{2}m_\pi}{\Lambda_\pi}\right)\Bigg\}\Bigg] \\
& +\lambda S_{12}\,(\boldsymbol{\tau}_1\cdot\boldsymbol{\tau}_2)\,\frac{m_\pi^2}{4\bar{M}M_N}\Bigg[\frac{2m_\pi^2}{\Lambda_\pi^2}\,\phi_T^0\left(m_\pi,\,\frac{\Lambda_\pi}{\sqrt{2}},\,r\right) \\
& -\frac{1}{6}\ (m_\pi r)\ \phi_V^0\left(m_\pi,\,\frac{\Lambda_\pi}{\sqrt{2}},\,r\right)\Bigg] \\
& +i\ (\boldsymbol{\sigma}_2\cdot\hat{\boldsymbol{r}})\,(\boldsymbol{\tau}_1\cdot\boldsymbol{\tau}_2)\,\frac{m_\pi}{2M_N}\Bigg[\left(1-\frac{m_\pi^2}{8\bar{M}^2}\right)\Bigg\{\frac{2m_\pi^2}{\Lambda_\pi^2}\,\phi_V^0\left(m_\pi,\,\frac{\Lambda_\pi}{\sqrt{2}},\,r\right) \\
& -\frac{1}{2}\ (m_\pi r)\ \phi_C^0\left(m_\pi,\,\frac{\Lambda_\pi}{\sqrt{2}},\,r\right)\Bigg\}-\frac{m_\pi^2}{8\bar{M}^2}\,\phi_V^0\left(m_\pi,\,\frac{\Lambda_\pi}{\sqrt{2}},\,r\right)\Bigg]\Bigg\}
\end{aligned} \tag{40}$$

2. $J^{PC} = 1^{++}$; $(\pi\sigma)$-pair exchange

$$\begin{aligned}
V^{(\mathrm{eff.2B})}_{(\pi\sigma)}(r) = {} & -\frac{4\pi\,\rho_{NM}}{m_\pi^3}\frac{g_{(\pi\sigma)}g_\pi^w}{4\pi}\frac{g_\sigma}{4\pi}\,2M_N\,\frac{m_\pi^2}{m_\sigma^2} \\
& \times\Bigg\{\lambda\,(\boldsymbol{\sigma}_1\cdot\boldsymbol{\sigma}_2)(\boldsymbol{\tau}_1\cdot\boldsymbol{\tau}_2)\,\frac{1}{3}\,\frac{m_\pi^2}{4\bar{M}M_N}\Bigg[\phi_C^1(m_\pi,\,\Lambda_\pi,\,r) \\
& +\frac{m_\pi^2}{4\bar{M}M_N}\,\phi_C^2(m_\pi,\,\Lambda_\pi,\,r)\Bigg] \\
& +\lambda S_{12}(\boldsymbol{\tau}_1\cdot\boldsymbol{\tau}_2)\frac{m_\pi^2}{4\bar{M}M_N}\Bigg[\phi_T^0(m_\pi,\,\Lambda_\pi,\,r)+\frac{m_\pi^2}{4\bar{M}M_N}\,\phi_T^1(m_\pi,\,\Lambda_\pi,\,r)\Bigg] \\
& +i\,(\boldsymbol{\sigma}_2\cdot\hat{\boldsymbol{r}})(\boldsymbol{\tau}_1\cdot\boldsymbol{\tau}_2)\frac{m_\pi}{2M_N}\Bigg[\phi_V^0(m_\pi,\,\Lambda_\pi,\,r)
\end{aligned}$$

$$
\begin{aligned}
&+\frac{m_\pi^2}{8\bar{M}M_N}\left\{\phi_V^0(m_\pi,\Lambda_\pi,r)-\frac{1}{2\sqrt{\pi}}\left(\frac{\Lambda_\pi}{m_\pi}\right)^4\left(\frac{\Lambda_\pi r}{2}\right)e^{-\left(\frac{\Lambda_\pi r}{2}\right)^2}\right\}\Bigg]\Bigg\}\\
&-\frac{4\pi\rho_{NM}}{m_\pi^3}\frac{G_F{m_\pi}^2}{4\pi}\frac{f_\pi g_\sigma}{4\pi}(2M_N)^2\frac{m_\pi}{m_\sigma^2}\\
&\times\Bigg\{A^{pc}_{(\pi\sigma)}(\boldsymbol{\sigma}_1\cdot\boldsymbol{\sigma}_2)(\boldsymbol{\tau}_1\cdot\boldsymbol{\tau}_2)\frac{1}{3}\frac{m_\pi^2}{4M_N^2}\Bigg[\phi_C^1(m_\pi,\Lambda_\pi,r)\\
&+\frac{m_\pi^2}{4\bar{M}M_N}\phi_C^2(m_\pi,\Lambda_\pi,r)\Bigg]+A^{pc}_{(\pi\sigma)}S_{12}(\boldsymbol{\tau}_1\cdot\boldsymbol{\tau}_2)\frac{m_\pi^2}{4{M_N}^2}\\
&\times\left[\phi_T^0(m_\pi,\Lambda_\pi,r)+\frac{m_\pi^2}{4\bar{M}M_N}\phi_T^1(m_\pi,\Lambda_\pi,r)\right]\Bigg\} \qquad (41)
\end{aligned}
$$

3. $J^{PC}=1^{+-}$; $(\pi\omega)$-pair exchange

$$
\begin{aligned}
V^{(\mathrm{eff.2B})}_{(\pi\omega)}(r)=&\ \frac{4\pi\rho_{NM}}{m_\pi^3}\frac{g_{(\pi\omega)}g_\pi^w}{4\pi}\frac{g_\omega}{4\pi}2M_N\frac{m_\pi^2}{m_\omega^2}\\
&\times\Bigg\{\lambda(\boldsymbol{\sigma}_1\cdot\boldsymbol{\sigma}_2)(\boldsymbol{\tau}_1\cdot\boldsymbol{\tau}_2)\left(1+\frac{1}{2M_N^2}\frac{3}{5}k_F^2\right)\frac{1}{3}\frac{m_\pi^2}{4\bar{M}M_N}\phi_C^1(m_\pi,\Lambda_\pi,r)\\
&+\lambda S_{12}(\boldsymbol{\tau}_1\cdot\boldsymbol{\tau}_2)\left(1+\frac{1}{2M_N^2}\frac{3}{5}k_F^2\right)\frac{m_\pi^2}{4\bar{M}M_N}\phi_T^0(m_\pi,\Lambda_\pi,r)\\
&+i(\boldsymbol{\sigma}_2\cdot\hat{\boldsymbol{r}})(\boldsymbol{\tau}_1\cdot\boldsymbol{\tau}_2)\frac{m_\pi}{2M_N}\Bigg[\left(1+\frac{1}{2M_N^2}\frac{3}{5}k_F^2\right)\phi_V^0(m_\pi,\Lambda_\pi,r)\\
&-\frac{m_\pi^2}{8\bar{M}M_N}\left\{\phi_V^0(m_\pi,\Lambda_\pi,r)-\frac{1}{2\sqrt{\pi}}\left(\frac{\Lambda_\pi}{m_\pi}\right)^4\left(\frac{\Lambda_\pi r}{2}\right)e^{-\left(\frac{\Lambda_\pi r}{2}\right)^2}\right\}\Bigg]\Bigg\}\\
&+\frac{4\pi\rho_{NM}}{m_\pi^3}\frac{G_F{m_\pi}^2}{4\pi}\frac{g_\omega}{4\pi}\frac{f_\pi}{m_\pi}2M_N2\bar{M}\frac{{m_\pi}^2}{m_\omega^2}\\
&\times\Bigg\{A^{pc}_{(\pi\omega)}(\boldsymbol{\sigma}_1\cdot\boldsymbol{\sigma}_2)(\boldsymbol{\tau}_1\cdot\boldsymbol{\tau}_2)\left(1-\frac{f_\omega}{g_\omega}\frac{1}{2M_N^2}\frac{3}{5}k_F^2\right)\\
&\times\frac{1}{3}\frac{m_\pi^2}{4\bar{M}M_N}\phi_C^1(m_\pi,\Lambda_\pi,r)\\
&+A^{pc}_{(\pi\omega)}S_{12}(\boldsymbol{\tau}_1\cdot\boldsymbol{\tau}_2)\left(1-\frac{f_\omega}{g_\omega}\frac{1}{2M_N^2}\frac{3}{5}k_F^2\right)\frac{m_\pi^2}{4\bar{M}M_N}\phi_T^0(m_\pi,\Lambda_\pi,r)\\
&-iB^{pv}_{(\pi\omega)}(\boldsymbol{\sigma}_2\cdot\hat{\boldsymbol{r}})(\boldsymbol{\tau}_1\cdot\boldsymbol{\tau}_2)\frac{m_\pi}{2M_N}\frac{m_\pi^2}{4\bar{M}^2}\Bigg[\phi_V^0(m_\pi,\Lambda_\pi,r).\\
&-\frac{1}{2\sqrt{\pi}}\left(\frac{\Lambda_\pi}{m_\pi}\right)^4\left(\frac{\Lambda_\pi r}{2}\right)e^{-\left(\frac{\Lambda_\pi r}{2}\right)^2}\Bigg]\Bigg\} \qquad (42)
\end{aligned}
$$

4. $J^P = 0^+$; $(K\pi)$-pair exchange

$$
\begin{aligned}
V^{(\mathrm{eff.2B})}_{(K\pi)}(r) = & -\frac{4\pi\rho_{NM}}{m_\pi^3}\frac{G_F {m_\pi}^2}{4\pi}\frac{g_{(K\pi)}}{4\pi}\frac{f_\pi}{m_\pi}2M_N m_\pi\frac{m_\pi^2}{m_K^2}\left[\frac{1}{2}C_K^{pv}+D_K^{pv}\right] \\
& \times\left\{ i\,(\boldsymbol{\sigma}_2\cdot\hat{\boldsymbol{r}})(\boldsymbol{\tau}_1\cdot\boldsymbol{\tau}_2)\frac{m_\pi}{2M_N}\left[\phi_V^0(m_\pi,\,\Lambda_\pi,\,r)\right.\right. \\
& \left.\left. -\frac{m_\pi^2}{8\bar{M}^2}\left\{\phi_V^0\,(m_\pi,\,\Lambda_\pi,\,r)-\frac{1}{2\sqrt{\pi}}\left(\frac{\Lambda_\pi}{m_\pi}\right)^4\left(\frac{\Lambda_\pi r}{2}\right)e^{-\left(\frac{\Lambda_\pi r}{2}\right)^2}\right\}\right]\right\} \\
& -\frac{4\pi\rho_{NM}}{m_\pi^3}\frac{G_F {m_\pi}^2}{4\pi}\frac{g_{\Lambda NK}}{4\pi}\frac{f_\pi}{m_\pi}2M_N m_\pi\left[\frac{1}{2}C_{K\pi}^{pc}\right] \\
& \times\left\{ (\boldsymbol{\sigma}_1\cdot\boldsymbol{\sigma}_2)(\boldsymbol{\tau}_1\cdot\boldsymbol{\tau}_2)\,\frac{1}{3}\left[\frac{m_\pi m_\pi}{m_K^2-m_\pi^2}\frac{m_\pi^2}{4\bar{M}M_N}\,\phi_C^1(m_\pi,\,\Lambda_\pi,\,r)\right.\right. \\
& \left.\left. -\frac{m_\pi m_K}{m_K^2-m_\pi^2}\frac{m_K^2}{4\bar{M}M_N}\,\phi_C^1(m_K,\,\Lambda_K,\,r)\right]\right. \\
& \left. + S_{12}(\boldsymbol{\tau}_1\cdot\boldsymbol{\tau}_2)\left[\frac{m_\pi m_\pi}{m_K^2-m_\pi^2}\frac{m_\pi^2}{4\bar{M}M_N}\phi_T^0(m_\pi,\,\Lambda_\pi,\,r)\right.\right. \\
& \left.\left. -\frac{m_\pi m_K}{m_K^2-m_\pi^2}\frac{m_K^2}{4\bar{M}M_N}\,\phi_T^0(m_K,\,\Lambda_K,\,r)\right]\right\} \qquad (43)
\end{aligned}
$$

5. $J^{PC} = 0^{++}$; $(\sigma\sigma)$-pair exchange

$$
\begin{aligned}
V^{(\mathrm{eff.2B})}_{(\sigma\sigma)}(r) = & \frac{4\pi\rho_{NM}}{m_\pi^3}\frac{G_F {m_\pi}^2}{4\pi}\frac{g_{(\sigma\sigma)}g_\sigma}{4\pi}\,m_\sigma\frac{{m_\pi}^2}{{m_\sigma}^2} \\
& \times\left\{ A_\sigma^{pc}\left[\phi_C^0\Big(m_\sigma,\,\frac{\Lambda_\sigma}{\sqrt{2}},\,r\Big)-\Big(1-\frac{{m_\sigma}^2}{4\bar{M}M_N}\Big)\right.\right. \\
& \times\left\{\Big(1+\frac{2m_\sigma^2}{\Lambda_\sigma^2}\Big)\,\phi_C^0\Big(m_\sigma,\,\frac{\Lambda_\sigma}{\sqrt{2}},\,r\Big)\right. \\
& -\frac{1}{4}\exp\big(2m_\sigma^2/\Lambda_\sigma^2\big)\Big[e^{-m_\sigma r}\mathrm{Erfc}\Big(-\frac{\Lambda_\sigma r}{2\sqrt{2}}+\frac{\sqrt{2}m_\sigma}{\Lambda_\sigma}\Big) \\
& \left.\left.+\,e^{m_\sigma r}\mathrm{Erfc}\Big(\frac{\Lambda_\sigma r}{2\sqrt{2}}+\frac{\sqrt{2}m_\sigma}{\Lambda_\sigma}\Big)\Big]\right\} \\
& \left.+\,\phi_C^0\,(m_\sigma,\,\Lambda_\sigma,\,r)-\frac{m_\sigma^2}{4\bar{M}M_N}\,\phi_C^1\,(m_\sigma,\,\Lambda_\sigma,\,r)\right] \\
& +i\,B_\sigma^{pv}\,(\boldsymbol{\sigma}_1\cdot\hat{\boldsymbol{r}})\,\frac{m_\sigma}{2M_N}\left[\frac{2m_\sigma^2}{\Lambda_\sigma^2}\,\phi_V^0\Big(m_\sigma,\,\frac{\Lambda_\sigma}{\sqrt{2}},\,r\Big)\right. \\
& \left.\left.-\frac{1}{2}\,(m_\sigma r)\,\phi_C^0\Big(m_\sigma,\,\frac{\Lambda_\sigma}{\sqrt{2}},\,r\Big)-\,\phi_V^0\,(m_\sigma,\,\Lambda_\sigma,\,r)\right]\right\} \\
& +\frac{4\pi\rho_{NM}}{m_\pi^3}\frac{G_F {m_\pi}^2}{4\pi}\frac{{g_\sigma}^2}{4\pi}\,m_\sigma\frac{{m_\pi}^2}{{m_\sigma}^2}
\end{aligned}
$$

$$\times \Bigg\{ A^{pc}_{(\sigma\sigma)} \left[\phi^0_C\left(m_\sigma,\, \Lambda_\sigma,\, r\right) - \frac{{m_\sigma}^2}{4\bar{M} M_N}\, \phi^1_C\left(m_\sigma,\, \Lambda_\sigma,\, r\right) \right] - i\, B^{pv}_{\sigma\sigma}\ \left(\boldsymbol{\sigma}_1 \cdot \hat{\boldsymbol{r}}\right)\, \frac{m_\sigma}{2M_N}\, \phi^0_V\left(m_\sigma,\, \Lambda_\sigma,\, r\right) \Bigg\} \tag{44}$$

6. Fujita–Miyazawa; $(\pi\pi)$-pair exchange

$$\begin{aligned} V^{(\text{eff.2B})}_{FM(\pi\pi)}(r) = {} & \frac{4\pi\,\rho_{NM}}{m_\pi^3} \frac{g^w_\pi}{4\pi} \frac{f_\pi}{4\pi} \frac{2M_N}{m_\pi}\, m_\pi \\ & \times \Bigg\{ \lambda\ (A+B)\ (\boldsymbol{\tau}_1 \cdot \boldsymbol{\tau}_2)\ \frac{m_\pi^2}{4\bar{M} M_N} \left[\frac{1}{3}\ (\boldsymbol{\sigma}_1 \cdot \boldsymbol{\sigma}_2)\ \phi^1_C\Big(m_\pi,\, \frac{\Lambda_F}{\sqrt{2}},\, r\Big) \right. \\ & \left. + S_{12}\, \phi^0_T\Big(m_\pi,\, \frac{\Lambda_F}{\sqrt{2}},\, r\Big) \right] + \lambda\ (A+B-D)\ (\boldsymbol{\tau}_1 \cdot \boldsymbol{\tau}_2) \\ & \times \frac{m_\pi^2}{4\bar{M} M_N} \Bigg[\frac{1}{3}\ (\boldsymbol{\sigma}_1 \cdot \boldsymbol{\sigma}_2) \Bigg\{ \left(1 + \frac{2m_\pi^2}{\Lambda_F^2}\right) \phi^0_C\Big(m_\pi,\, \frac{\Lambda_F}{\sqrt{2}},\, r\Big) \\ & - \frac{1}{4} \exp\left(2m_\pi^2/\Lambda_F^2\right) \Bigg[e^{-m_\pi r} \mathrm{Erfc}\Big(-\frac{\Lambda_F r}{2\sqrt{2}} + \frac{\sqrt{2} m_\pi}{\Lambda_F}\Big) \\ & + e^{m_\pi r} \mathrm{Erfc}\Big(\frac{\Lambda_F r}{2\sqrt{2}} + \frac{\sqrt{2} m_\pi}{\Lambda_F}\Big) \Bigg] \Bigg\} \\ & + S_{12} \left\{ \frac{2m_\pi^2}{\Lambda_F^2}\, \phi^0_T\Big(m_\pi,\, \frac{\Lambda_F}{\sqrt{2}},\, r\Big) - \frac{1}{6}\ (m_\pi r)\ \phi^0_V\Big(m_\pi,\, \frac{\Lambda_F}{\sqrt{2}},\, r\Big) \right\} \Bigg] \\ & + i\ (A+B)\ (\boldsymbol{\sigma}_2 \cdot \hat{\boldsymbol{r}})\, (\boldsymbol{\tau}_1 \cdot \boldsymbol{\tau}_2)\ \frac{m_\pi}{2M_N}\, \phi^0_V\Big(m_\pi,\, \frac{\Lambda_F}{\sqrt{2}},\, r\Big) \\ & + i\ (A+B-D)\ (\boldsymbol{\sigma}_2 \cdot \hat{\boldsymbol{r}})\, (\boldsymbol{\tau}_1 \cdot \boldsymbol{\tau}_2)\, \frac{m_\pi}{2M_N} \Bigg[\frac{2m_\pi^2}{\Lambda_F^2}\, \phi^0_V\Big(m_\pi,\, \frac{\Lambda_F}{\sqrt{2}},\, r\Big) \\ & - \frac{1}{2}\ (m_\pi r)\ \phi^0_C\Big(m_\pi,\, \frac{\Lambda_F}{\sqrt{2}},\, r\Big) \Bigg] \Bigg\} \end{aligned} \tag{45}$$

In the above expressions, $\phi^0_C(m,\, \Lambda,\, r)$, $\phi^1_C(m,\, \Lambda,\, r)$, $\phi^2_C(m,\, \Lambda,\, r)$, $\phi^0_T(m,\, \Lambda,\, r)$, and $\phi^1_T(m,\, \Lambda,\, r)$, are defined in Ref. [23], and

$$\begin{aligned} \phi^0_V\left(m,\, \Lambda,\, r\right) = {} & \Bigg\{ \exp\left(m^2/\Lambda^2\right) \Bigg[(1+mr)\, e^{-mr}\, \mathrm{Erfc}\Big(-\frac{\Lambda r}{2} + \frac{m}{\Lambda}\Big) \\ & - (1-mr)\, e^{mr}\, \mathrm{Erfc}\Big(\frac{\Lambda r}{2} + \frac{m}{\Lambda}\Big) \Bigg] \\ & - \frac{4}{\sqrt{\pi}} \Big(\frac{\Lambda r}{2}\Big) \exp\Bigg[- \Big(\frac{\Lambda r}{2}\Big)^2 \Bigg] \Bigg\} / 2\,(mr)^2\,. \end{aligned} \tag{46}$$

$\mathrm{Erfc}(x)$ is a complimentary error function defined as

$$\mathrm{Erfc}(x) = \frac{2}{\sqrt{\pi}} \int_x^\infty e^{-t^2} dt. \tag{47}$$

4. Weak coupling constants for the ΛN-(meson-pair) and weak Λ–n mixing model

Although the ESC model gives strong coupling constants for the NN-(meson-pair) vertices, it does not give weak coupling constants for the ΛN-(meson-pair) ones. This matter is discussed in this section.

4.1 *Weak Λ–n mixing model*

Following the Dalitz–Von Hippel method [31], we consider the weak Λ–n mixing. The physical n and Λ are the mixtures

$$\begin{pmatrix} n \\ \Lambda \end{pmatrix} = \begin{pmatrix} \cos\varepsilon & -\sin\varepsilon \\ \sin\varepsilon & \cos\varepsilon \end{pmatrix} \begin{pmatrix} n^0 \\ \Lambda^0 \end{pmatrix}, \tag{48}$$

where n^0 and Λ^0 are respectively the unphysical bare states, eigenstates of I (isospin) and S (strangeness).

The mass matrix on the "bare" basis is

$$H = \begin{pmatrix} M_n^0 & \Delta \\ \Delta & M_\Lambda^0 \end{pmatrix}, \tag{49}$$

and Δ is given by the transition matrix element of the weak mixing interaction

$$\Delta = \left\langle n^0 \,|H_I^w|\, \Lambda^0 \right\rangle. \tag{50}$$

From the mass matrix of Eq. (49), one obtains the states $|n>$ and $|\Lambda>$ and the masses M_n and M_Λ. Since $\Delta, \varepsilon \ll 1$, one gets

$$|n\rangle = |n^0\rangle - \varepsilon\,|\Lambda^0\rangle, \quad |\Lambda\rangle = |\Lambda^0\rangle + \varepsilon\,|n^0\rangle, \tag{51}$$

where

$$\tan\varepsilon \approx \varepsilon = -\frac{\Delta}{\Delta M}, \quad \Delta M = M_n - M_\Lambda. \tag{52}$$

The physical masses in terms of the bare masses are

$$M_\Lambda = M_\Lambda^0 - \frac{\Delta^2}{\Delta M}, \quad M_n = M_n^0 + \frac{\Delta^2}{\Delta M}. \tag{53}$$

4.2 *Estimate of the mixing angle ε and internal π-exchange $\Lambda \to n$ transition*

Since the mixing angle ε is given by Eq. (52), one must evaluate the transition matrix element $\Delta_\Lambda \equiv \Delta$ of Eq. (50):

$$\Delta_\Lambda = \left\langle n^0 \,|\sum_{i,j} V^\pi_{Q_iQ_j}|\, \Lambda^0 \right\rangle. \tag{54}$$

$|n^0>$ and $|\Lambda^0>$ are the neutron and Λ wave function, respectively, in the non-relativistic quark model. $V^\pi_{Q_iQ_j}$ signifies the weak pion-exchange quark–quark interaction.

The quark–quark weak interaction Hamiltonian of one-pion exchange, for the dominant parity-conserving part, is

$$\mathcal{H}^{(w)}_{QQ\pi} = -\frac{f^{(w)}_{QQ\pi}}{m_{\pi^+}} (\bar\Psi_N \gamma_\mu \gamma_5 \boldsymbol{\tau} \Psi_S) \cdot \partial^\mu \boldsymbol{\varphi}_\pi, \tag{55}$$

and the strong interaction Hamiltonian is

$$\mathcal{H}^{(s)}_{QQ\pi} = -\frac{f^{(s)}_{QQ\pi}}{m_{\pi^+}} (\bar\Psi_N \gamma_\mu \gamma_5 \boldsymbol{\tau} \Psi_N) \cdot \partial^\mu \boldsymbol{\varphi}_\pi. \tag{56}$$

Here

$$\Psi_N = \begin{pmatrix} \psi_u \\ \psi_d \end{pmatrix} \quad \text{and} \quad \Psi_S = \begin{pmatrix} 0 \\ \psi_s \end{pmatrix}, \tag{57}$$

where Ψ_S is a spurion.

When the Gaussian form factor of the type $\exp(-\boldsymbol{k}^2/2\Lambda_{QQ}^2)$ with a cut-off mass Λ_{QQ} is considered at the quark–quark–pion vertex, the one-pion exchange potential in the configuration space is obtained, except the tensor part[1], as

$$V^{(\pi)}_{Q_iQ_j}(r) = \frac{f^{(w)}_{QQ\pi} f^{(s)}_{QQ\pi}}{4\pi} \left(\frac{m_\pi^3}{m_{\pi^+}^2}\right) \frac{1}{3}(\boldsymbol{\sigma}_i \cdot \boldsymbol{\sigma}_j)(\boldsymbol{\tau}_i \cdot \boldsymbol{\tau}_j)\, \phi^1_C(m_\pi, \Lambda_{QQ}, r), \tag{58}$$

with

$$\phi^1_C(m_\pi, \Lambda_{QQ}, r) = \phi^0_C(m_\pi, \Lambda_{QQ}, r) - \frac{1}{2\sqrt{\pi}} \left(\frac{\Lambda_{QQ}}{m_\pi}\right)^3 e^{-\frac{1}{4}\Lambda^2_{QQ} r^2}. \tag{59}$$

In Eq. (59) the first term on the r.h.s. defines the "Yukawa" part potential, and the second term the "cut-off" part one. Here we concentrate on the "Yukawa"-type potential and ignore the "cut-off" part, because the "cut-off" part is independent of the exchanged-meson mass and is expected to be small due to cancellation when various meson exchanges such as π, K, η, η',… are considered.

For the internal pseudo-scalar meson exchange, we are interested only in the region of $r \leq 0.5$ fm, and we expand $\phi^0_C(m, \Lambda_{QQ}, r)$ in the Taylor series and approximate the potential in this region by a Gaussian such that

$$\phi^0_C(m_\pi, \Lambda_{QQ}, r) \approx \phi^0_C(m_\pi, \Lambda_{QQ}, r=0)\, e^{-\frac{1}{4}U^2 r^2}, \tag{60}$$

$$U = \sqrt{-2\phi^{0\,\prime\prime}_C(r=0)/\phi^0_C(r=0)}. \tag{61}$$

With this approximation, one gets

$$V^{(\pi)}_{Q_iQ_j}(r) = V_0\, (\boldsymbol{\sigma}_i \cdot \boldsymbol{\sigma}_j)(\boldsymbol{\tau}_i \cdot \boldsymbol{\tau}_j)\, e^{-\frac{1}{4}U^2 r^2} \tag{62}$$

and

$$V_0 = \frac{1}{3} \frac{f^{(w)}_{QQ\pi} f^{(s)}_{QQ\pi}}{4\pi} \left(\frac{m_\pi^3}{m_{\pi^+}^2}\right) \phi^0_C(m_\pi, \Lambda_{QQ}, r=0). \tag{63}$$

Now, to estimate the size of the potential we replace the potential (62) by a constant potential $\bar{V}^{(\pi)}_{Q_iQ_j}(r)$ for $r < R$ and 0 for $r \geq R$, where R is a effective baryon radius (≈ 0.5 fm) under the condition of volume-integral-equivalence for the two potentials $V^{(\pi)}_{Q_iQ_j}(r)$ and $\bar{V}^{(\pi)}_{Q_iQ_j}(r)$.

Then

$$\begin{aligned} \bar{V}^{(\pi)}_{Q_iQ_j}(r) &= V_0\, (\boldsymbol{\sigma}_i \cdot \boldsymbol{\sigma}_j)(\boldsymbol{\tau}_i \cdot \boldsymbol{\tau}_j)\, g_0 \theta(R-r) \\ &= \bar{V}_0\, (\boldsymbol{\sigma}_i \cdot \boldsymbol{\sigma}_j)(\boldsymbol{\tau}_i \cdot \boldsymbol{\tau}_j)\, \theta(R-r), \end{aligned} \tag{64}$$

and

$$\bar{V}_0 = \frac{f^{(w)}_{QQ\pi} f^{(s)}_{QQ\pi}}{4\pi} \frac{m_{\pi^+}}{(m_{\pi^+}R)^3} \left(\frac{m_\pi}{U}\right)^3 2\sqrt{\pi}\, \phi^0_C(m_\pi, \Lambda_{QQ}, r=0). \tag{65}$$

The quark–quark–pion coupling constants are related to the baryon–baryon–pion ones, which read [32] as

[1]The tensor interaction is not included here, since it does not induce the $\Lambda \to n$ transition.

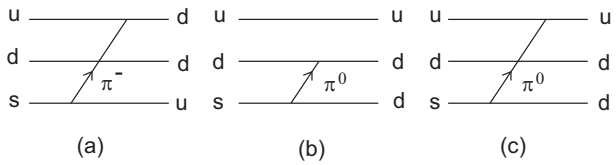

Fig. 2. Feynman diagrams for the internal pion exchange weak $\Lambda^0 \to n^0$ transitions among quark lines.

$$f^{(w)}_{QQ\pi} = \frac{3}{5} f^{(w)}_{\Lambda N\pi} = \frac{3}{5} \frac{m_\pi}{2\bar{M}} g^{(w)}_{\Lambda N\pi}, \tag{66}$$

$$f^{(s)}_{QQ\pi} = \frac{3}{5} f^{(s)}_{NN\pi} = \frac{3}{5} \frac{m_\pi}{2M_N} g^{(s)}_{NN\pi}. \tag{67}$$

$|n^0>$ and $|\Lambda^0>$ are expressed in SU(6) quark wave functions:

$$\begin{aligned}\Psi(n^0) = {} & \Phi_{n^0}(\text{Color singlet})\, \phi_{n^0}(\,(0s)^3\, L = M = 0) \\ & \times \psi_{n^0}(\,ud^2, \mathbf{8},\ I = 1/2, I_z = -1/2,\ S = S_z = 1/2),\end{aligned} \tag{68}$$

$$\begin{aligned}\Psi(\Lambda^0) = {} & \Phi_{\Lambda^0}(\text{Color singlet})\, \phi_{\Lambda^0}(\,(0s)^3\, L = M = 0) \\ & \times \psi_{\Lambda^0}(\,ud's', \mathbf{8},\ I =' 1/2', I_z =' -1/2',\ S = S_z = 1/2).\end{aligned} \tag{69}$$

In Eqs. (68) and (69), the color part of the wave functions is completely antisymmetric for the exchanges of quarks, while the space–flavor–spin part is completely symmetric. Further, in Eq. (69), the s-quark is treated as $'s'$, which has weak-isospin quantum numbers $i = '1/2' i_z = ' - 1/2'$, since it is a spurion. We assign the index 3 to the s-quark.

Then the matrix element of Δ_Λ in Eq. (54) is

$$\begin{aligned}\Delta_\Lambda = {} & \left\langle n^0 \,|\, \sum_{i,j} \bar{V}^\pi_{QQ}(i,j) \,|\, \Lambda^0 \right\rangle \\ = {} & 2\,\langle\, n^0 \,|\bar{V}^\pi_{QQ}(1,3)\,|\,\Lambda^0\,\rangle \\ = {} & 2\,\langle\, \Phi_{n^0}(\text{Color singlet}) \,|\, \Phi_{\Lambda^0}(\text{Color singlet})\,\rangle \\ & \times \langle \phi_{n^0}(\,(0s)^3\, L' = M' = 0) \,|\, \bar{V}_0\theta(R - r_{13})\,|\phi_{\Lambda^0}(\,(0s)^3\, L = M = 0)\,\rangle \\ & \times \langle\, \psi_{n^0}(\,ud^2, \mathbf{8},\ I' = 1/2, I'_z = -1/2,\ S' = S'_z = 1/2)\,|(\boldsymbol{\sigma}_1 \cdot \boldsymbol{\sigma}_3)(\boldsymbol{\tau}_1 \cdot \boldsymbol{\tau}_3)\,\delta(q_3, s)\,| \\ & \times \psi_{\Lambda^0}(\,ud's', \mathbf{8},\ I =' 1/2', I_z =' -1/2',\ S = S_z = 1/2)\,\rangle.\end{aligned} \tag{70}$$

Figures 2(a)–(c) show the Feynman diagrams for the internal pion exchange weak $\Lambda^0 \to n^0$ transitions that give an intuitive insight into Eq. (70).

As for the color part in Eq. (70), the overlap matrix element is 1, and for the spacial part matrix element we take

$$\langle \phi_{n^0}(\,(0s)^3\, L' = M' = 0) \,|\, \bar{V}_0\theta(R - r_{13})\,|\phi_{\Lambda^0}(\,(0s)^3\, L = M = 0)\,\rangle \ \approx\ \bar{V}_0 \tag{71}$$

in an approximation that the spacial wave function of the $(0s)$ state is of short enough range compared with R $(=\ 0.5$ fm).

The $(\boldsymbol{\sigma}_1 \cdot \boldsymbol{\sigma}_3)(\boldsymbol{\tau}_1 \cdot \boldsymbol{\tau}_3)$-operator matrix element is evaluated as

$$\begin{aligned}\text{M.E.} &= \langle\, \psi_{n^0}(\, ud^2, \mathbf{8},\ I' = 1/2, I'_z = -1/2,\ S' = S'_z = 1/2)\,|(\boldsymbol{\sigma}_1 \cdot \boldsymbol{\sigma}_3)(\boldsymbol{\tau}_1 \cdot \boldsymbol{\tau}_3)\,\delta(q_3, s)\,| \\ &\quad \times\, \psi_{\Lambda^0}(\, ud\,'s', \mathbf{8},\ I =' 1/2', I_z =' -1/2',\ S = S_z = 1/2)\,\rangle \\ &= \frac{1}{2}\sqrt{2\cdot 3}. \end{aligned} \tag{72}$$

Finally we get

$$\Delta_\Lambda \cong\ 2\,\bar{V}_0\,\frac{1}{2}\,\sqrt{2\cdot 3}. \tag{73}$$

From Eq. (52), with Eqs. (65)–(67) and (73), we obtain the mixing angle ε as

$$\begin{aligned}\varepsilon = &-\frac{9}{25}\frac{g^{(w)}_{\Lambda N\pi} g^{(s)}_{NN\pi}}{4\pi}\left(\frac{m_\pi}{2\bar{M}}\right)\left(\frac{m_\pi}{2M_N}\right)\frac{m_{\pi^+}}{M_N - M_\Lambda} \\ &\times \frac{1}{(m_{\pi^+}R)^3}\left(\frac{m_\pi}{U}\right)^3 2\sqrt{\pi}\,\sqrt{2\cdot 3}\,\phi^0_C(m_\pi, \Lambda_{QQ}, r=0). \end{aligned} \tag{74}$$

4.3 *Weak ΛN-(meson-pair) coupling constants*

One can evaluate the weak ΛN-(meson-pair) coupling constant of a Hamiltonian, for the parity-conserving (pc) part, in the Λ–n weak mixing model. In this model the weak transition proceeds in a way that in the course of internal transmutation from Λ to n taking place the strong baryon–baryon–(meson-pair) interaction emerges, or inversely that the strong baryon–baryon–(meson-pair) interaction works accompanying the slow weak transmutation from Λ to n. We may write

$$\left\langle n\,|H^{(w)}_{(\text{meson-pair})}\,|\,\Lambda\right\rangle = \text{Weak mixing part of}\ \left\langle n^0 - \varepsilon\,\Lambda^0\ |\,H^{(s)}_{(\text{meson-pair})}\,|\,\Lambda^0 + \varepsilon\, n^0\right\rangle \tag{75}$$

$$= \varepsilon\left\langle n^0\,|H^{(s)}_{(\text{meson-pair})}\,|\,n^0\right\rangle, \tag{76}$$

if the meson pair is an isovector. This leads to

$$g^{(w)}_{\Lambda n(\text{meson-pair})}\,(\text{pc part})\ =\ \varepsilon\, g^{(s)}_{nn(\text{meson-pair})}. \tag{77}$$

In the case that the isospin independence holds in the strong interaction and the $\Delta I = 1/2$ rule holds in the weak one, Eq. (77) is generalized to

$$g^{(w)}_{\Lambda N(\text{meson-pair})}\,(\text{pc part})\ =\ \varepsilon\, g^{(s)}_{NN(\text{meson-pair})}. \tag{78}$$

Then we obtain

$$g^{(w)}_{\Lambda N(\pi\sigma)}\,(\text{pc part}) \equiv G_F m_\pi^2\, A^{pc}_{(\pi\sigma)}\ =\ \varepsilon\, g_{(\pi\sigma)}, \tag{79}$$

$$g^{(w)}_{\Lambda N(\pi\omega)}\,(\text{pc part}) \equiv G_F m_\pi^2\, A^{pc}_{(\pi\omega)}\ =\ \varepsilon\, g_{(\pi\omega)}. \tag{80}$$

When the exchanged meson pair is iso-scalar such as $(\pi\pi)_0$ and $(\sigma\sigma)$, the following relations hold:

$$g^{(w)}_{\Lambda N(\pi\pi)_0}\,(\text{pc part}) \equiv G_F m_\pi^2\, A^{pc}_{(\pi\pi)_0}\ =\ \varepsilon\,(g_{(\pi\pi)_0}\ -\ g_{\Lambda\Lambda(\pi\pi)_0}), \tag{81}$$

$$g^{(w)}_{\Lambda N(\sigma\sigma)}\,(\text{pc part}) \equiv G_F m_\pi^2\, A^{pc}_{(\sigma\sigma)}\ =\ \varepsilon\,(g_{(\sigma\sigma)}\ -\ g_{\Lambda\Lambda(\sigma\sigma)}). \tag{82}$$

Since we have, however, no information about $g_{\Lambda\Lambda(\pi\pi)_0}$ and $g_{\Lambda\Lambda(\sigma\sigma)}$, we neglect those.

5. Estimate of two-nucleon induced decay rates with use of effective two-body $\Lambda N \to NN$ potentials

In Sect. 3 the effective two-body potentials $V^{(\mathrm{eff.2B})}(\Lambda N\text{–}NN)$ are deduced from weak three-body interactions for $\Lambda NN \to NNN$ transitions. We apply these effective potentials $V^{(\mathrm{eff.2B})}$ to evaluate the non-mesonic decay rates of hypernuclei. However, since the potentials $V^{(\mathrm{eff.2B})}(\Lambda N\text{–}NN)$ have a different origin from the usual two-body $V(\Lambda N\text{–}NN)$ such as meson-exchange potentials, it is not appropriate to sum up the potentials $V(\Lambda N\text{–}NN)$ and $V^{(\mathrm{eff.2B})}(\Lambda N\text{–}NN)$ beforehand to evaluate the decay rate. On the other hand, the sum of the decay rates $\Gamma_{nm}(\Lambda N \to NN) + \Gamma_{nm}^{(\mathrm{eff.2B})}(\Lambda N \to NN)$ is meaningful because the two decay channels are independent of each other, as explained. We designate $\Gamma_{nm}^{(\mathrm{eff.2B})}$ for the decay rate calculated with the use of the $V^{(\mathrm{eff.2B})}$ potentials. The decay rate $\Gamma_{nm}^{(\mathrm{eff.2B})}$ can be calculated in the standard shell model framework by adopting $V^{(\mathrm{eff.2B})}(\Lambda N\text{–}NN)$ for the transition potential. The expression of Γ_{nm} in the shell model basis is given in Eq. (3) of Ref. [6] and Eq. (2.9) of Ref. [5].

$\Gamma_{nm}^{(\mathrm{eff.2B})}$ is the sum of the proton-stimulated decay rate $\Gamma_{p}^{(\mathrm{eff.2B})}(\Lambda p \to np)$ and the neutron-stimulated one $\Gamma_{n}^{(\mathrm{eff.2B})}(\Lambda n \to nn)$ as

$$\Gamma_{nm}^{(\mathrm{eff.2B})} = \Gamma_{p}^{(\mathrm{eff.2B})}(\Lambda p \to np) + \Gamma_{n}^{(\mathrm{eff.2B})}(\Lambda n \to nn). \tag{83}$$

Hereafter, we use the shortened notations $\Gamma_{p}^{(\mathrm{eff.2B})}$ and $\Gamma_{n}^{(\mathrm{eff.2B})}$ for $\Gamma_{p}^{(\mathrm{eff.2B})}(\Lambda p \to np)$ and $\Gamma_{n}^{(\mathrm{eff.2B})}(\Lambda n \to nn)$, respectively. Although $\Gamma_{p}^{(\mathrm{eff.2B})}$ and $\Gamma_{n}^{(\mathrm{eff.2B})}$ are decay rates calculated for the two-body decay, the sum $\Gamma_{nm}^{(\mathrm{eff.2B})}$ in Eq. (83) would partly simulate the decay rate of Γ_{2N}, which is the sum of $\Gamma_{np}(\Lambda np \to nnp)$, $\Gamma_{pp}(\Lambda pp \to npp)$, and $\Gamma_{nn}(\Lambda nn \to nnn)$. It is one of the objects of this paper to evaluate the decay rate $\Gamma_{nm}^{(\mathrm{eff.2B})}$ as an "order of magnitude" of the two-nucleon induced decay rate.

It should be mentioned here that our calculation of the decay rate is based on the two-body dynamics, not on the full three-body one, and therefore our "effective two-body potential method" has certain limitations. First we would like to note the limitation in the deduction procedure of the effective two-body potentials. As is seen in Eq. (34), we derive $V^{(\mathrm{eff.2B})}(1, 2)$ by integrating over the particle-"3" variables (space, isospin, and spin degrees) of the three-body interaction $V^{\mathrm{W3B}}(\boldsymbol{x}_1, \boldsymbol{x}_2, \boldsymbol{x}_3)$ with use of the LNR approximation. In the procedure of the LNR approximation, especially owing to operations on $Tr(\boldsymbol{\tau}_3)$ and $Tr(\boldsymbol{\sigma}_3)$, the contributions from the possibly important three-body interactions due to, for instance, $(\pi\pi)_1$, $(\pi\eta)$, and $(\pi\rho)_1$ exchanges, are vanishing, as already shown in Sect. 3.2. At the present stage, however, we have no reliable way of evaluating such lost diagrams. Therefore, we know that the effects of the three-body interactions on the non-mesonic decay rates should surely be different between the two cases, the case of treating the full three-body dynamics, if possible, and the case of the approximation method through the form of effective two-body potentials.

Second, the decay kinematics is decisively different between the full treatment of the three-body decay and the approximate one in the two-body dynamics with effective two-body potentials. In the former, the final three nucleons share the energy of the decay Q-value among them and a particular nucleon pair does not carry definite energy, while in the latter treatment the final pair of nucleons have definite energy determined by the two-body kinematics. As a result, the relative momenta of the final pair of nucleons (np, pp, and nn among NNN) become different from the case of the two-body decay, which has a vital effect on the decay rate.

Considering the above-mentioned limitations at the present stage, it is conceivable that (i) the calculated $\Gamma_{nm}^{(\mathrm{eff.2B})}$ in our "effective two-body potential method" should give a limited

estimate of the two-nucleon induced non-mesonic decay rate, but (ii) the ratio of the two-nucleon induced partial decay rates as $\Gamma_{np} : \Gamma_{pp} : \Gamma_{nn}$ cannot be accounted for from $\Gamma_p^{(\mathrm{eff.2B})}$ and $\Gamma_n^{(\mathrm{eff.2B})}$.

6. Results and discussions

6.1 *Hypernuclear and nuclear wave functions, and coupling constants of meson-pair exchange Hamiltonians*

In evaluation of the non-mesonic decay rate, we employ the Λ-hypernuclear state in which a Λ-hyperon in the 0*s* state is coupled to the core-nucleus. The Λ-hyperon state is solved in the cluster model of Λ plus core-nucleus for ${}^{5}_{\Lambda}$He, while it is solved in the DDHF equation for the *p*-shell hypernuclei. For the core-nucleus part of the initial Λ-hypernucleus and the final daughter nuclei, the harmonic oscillator (HO) shell model wave functions are used. For the *p*-shell case, two types of HO shell model wave functions, the simple HO ones or the Cohen–Kurath-type configuration-mixed HO ones, are used. We solve the scattering state for the outgoing two nucleons for which the strong *NN* interactions act as the final-state correlation. The details are described in our previous works [5,6].

The *NN*-(meson-pair) coupling constants in the strong interaction Hamiltonians of Eqs. (1)–(7) have been determined and modified to be consistent with baryon–baryon–meson ones in explaining the *NN*- and *YN*-scattering data in several versions of the Nijmegen ESC [23–27] and GESC models [28]. Uncertainties exist in the relative magnitudes between various meson-pair exchange coupling constants. In the ESC and GESC models, $g_{(\pi\pi)_0}$ is set to be 0 (which results mostly from cancellation due to the σ- and pomeron-contribution effect), and no attempt has been made to fix $g_{(K\pi)}$ yet.

We designate the set of strong meson-pair coupling constants adopted in Refs. [28], [23], [24,25], and [26,27] as E15, E10, E16, and E19, respectively. As for the coupling constant $g_{(\sigma\sigma)}$, several values are used as a free parameter [28]. The coupling constants A, B, and D in Eq. (9) are taken from the original paper [19], i.e., $A = \frac{5\pi}{18} \cdot (3.70)$, $B = \frac{3}{5} A$, and $D = \frac{2\pi}{3} \cdot (-0.06)$. Note that A and B are in units of m_π^{-3}, and D is in units of m_π^{-1}.

The meson-pair coupling constants in the strong interactions adopted in this paper are listed in Table 1, where the rationalized representation (the scaling mass in the Hamiltonian is taken to be m_π) is used.

The weak meson-pair coupling constants, for their parity-conserving part, in the weak interaction Hamiltonians in Eqs. (10), (12), (15), and (16) can be determined by the relations in Eqs. (81), (82), (79), and (80), respectively. We do not try to determine the weak *NN*–($K\pi$) coupling constants here.

The weak mixing angle ε must be evaluated first from Eq. (74). $g^w_{\Lambda N\pi} = g^w \lambda = 0.233 \times 10^{-6} \times (-6.87)$ and $g^s_{NN\pi} = 12.807$ are adopted [6]. We take $m_\pi = m_{\pi^+}$ and $R = 0.5$ fm. U is determined by Eq. (61) and depends on m_π and Λ_{QQ} through a function $\phi^0_C(m_\pi, \Lambda_{QQ}, r = 0)$. Two choices, $\Lambda_{QQ} = 250\,\mathrm{MeV}/c^2$ and $\Lambda_{QQ} = 400\,\mathrm{MeV}/c^2$, are considered. Then we have

(1) $\Lambda_{QQ} = 250\,\mathrm{MeV}/c^2$ case: $U = 192\,\mathrm{MeV}/c^2$ and $\varepsilon = -0.758 \times 10^{-7}$ are obtained,
(2) $\Lambda_{QQ} = 400\,\mathrm{MeV}/c^2$ case: $U = 285\,\mathrm{MeV}/c^2$ and $\varepsilon = -0.496 \times 10^{-7}$ are obtained.

Since $\Lambda_{QQ} = 250\,\mathrm{MeV}/c^2$ is close to Λ_{QCD} and seems plausible for short-range behavior, we accept this choice and take $\varepsilon = -0.758 \times 10^{-7}$ for the Λ–*n* mixing angle in the following

Table 1. Strong and weak meson-pair coupling constants. The strong meson-pair coupling constants are taken from the ESC and GESC models. The coupling constants marked (*) have signs opposite to those given in ESC and GESC models due to the definition of the Hamiltonian (6). Fujita–Miyazawa $(\pi\pi)$-pair coupling constants A and B are given in units of ${m_\pi}^{-3}$, and D is given in units of ${m_\pi}^{-1}$. The weak coupling constants are shown for the weak mixing angle $\varepsilon = -0.758 \times 10^{-7}$, and are given in units of $G_F m_\pi^2 = 0.222 \times 10^{-6}$. See the text for symbols.

	Ref. [28] E15	Ref. [23] E10	Refs. [24,25] E16	Refs. [26,27] E19	Ref. [28]	Ref. [19]
Strong						
$g_{(\pi\pi)_0}$	–	–	–	–		
$g_{(\pi\sigma)}$	0.5509 (*)	0.1734 (*)	0.5519 (*)	0.7208 (*)		
$g_{(\pi\omega)}$	−0.6005	−0.6824	−0.1030	−0.6077		
$g_{(K\pi)}$	–	–	–	–		
$g_{(\sigma\sigma)}$ (a)					−1.885	
$g_{(\sigma\sigma)}$ (b)					−3.770	
$g_{(\sigma\sigma)}$ (c)					−4.084	
A						0.327
B						0.196
D						−0.126
Weak						
$A^{pc}_{(\pi\pi)_0}$	–	–	–	–		
$A^{pc}_{(\pi\sigma)}$	−0.1880	−0.0592	−0.1880	−0.2460		
$A^{pc}_{(\pi\omega)}$	0.2050	0.2330	0.0352	0.2070		
$C^{pc}_{(K\pi)}$	–	–	–	–		
$D^{pc}_{(K\pi)}$	–	–	–	–		
$A^{pc}_{(\sigma\sigma)}$ (a)					0.643	
$A^{pc}_{(\sigma\sigma)}$ (b)					1.287	
$A^{pc}_{(\sigma\sigma)}$ (c)					1.394	

discussion. Then the weak meson-pair coupling constants are fixed and are shown in accordance with the strong meson-pair coupling constants in Table 1.

The strong coupling constants of NN–meson and ΛNK, and the weak ones of ΛN–meson and NNK are the same as those adopted in Ref. [6]. Only the weak $\Lambda N\sigma$ coupling constants are determined phenomenologically so that the weak $\Lambda N \to NN$ potential due to the one-σ exchange can simulate the weak one due to the $2\pi/\sigma$ exchange as well as possible, i.e.,

$$V_\sigma^{\rm weak}(\Lambda N - NN) \approx V^{\rm weak}_{2\pi/\sigma(A+B)}(\Lambda N - NN), \tag{84}$$

where $V^{\rm weak}_{2\pi/\sigma(A+B)}(\Lambda N - NN)$ has been calculated in Ref. [6]. Then $A_\sigma^{pc} = -6.420$ and $B_\sigma^{pv} = 0.260$ are determined in units of $G_F m_\pi^2$.

As mentioned before, the Gaussian form factors $F(\boldsymbol{k}^2) = \exp(-\boldsymbol{k}^2/\Lambda_m^2)$ are used in deriving $V^{\rm (eff.2B)}(\Lambda N$–$NN)$. The cut-off mass Λ_m for the meson m $(m = \pi,\ K,\ \sigma)$ is taken to be $\Lambda_m = 1029.42$ MeV, and for Λ_F in Fujita–Miyazawa $(\pi\pi)$ exchange $\Lambda_F = 2000.0$ MeV is adopted.

6.2 *Non-mesonic decay rates* $\Gamma_{nm}^{\rm (eff.2B)}$

$\Gamma_{nm}^{\rm (eff.2B)}$ has a different origin concerning the decay transition potentials from the usual one-nucleon induced decay rate Γ_{nm} as stated in Sect. 5, and we like to regard $\Gamma_{nm}^{\rm (eff.2B)}$ as the "order of magnitude" of the two-nucleon induced non-mesonic decay rate Γ_{2N} and compare the

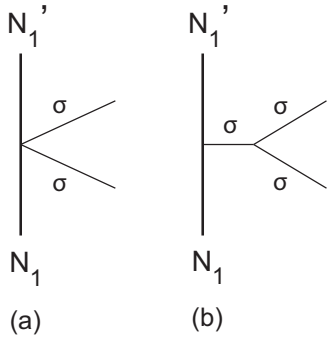

Fig. 3. Feynman diagrams of the scalar $(\sigma\sigma)$-pair coupling to N. (a) N couples directly to the $(\sigma\sigma)$ pair. (b) N couples to σ followed by $\sigma \to \sigma + \sigma$.

calculated $\Gamma_{nm}^{(\mathrm{eff.2B})}$ with experiments. We call these collectively the effective non-mesonic decay rates for $\Gamma_{p}^{(\mathrm{eff.2B})}$, $\Gamma_{n}^{(\mathrm{eff.2B})}$, and $\Gamma_{nm}^{(\mathrm{eff.2B})}$.

The effective non-mesonic decay rates are evaluated for hypernuclei ${}^{5}_{\Lambda}$He, ${}^{11}_{\Lambda}$B, and ${}^{12}_{\Lambda}$C, for which experimental data on Γ_{2N} exist.

As stated in Sect. 6.1, the coupling constants of the $(\pi\pi)_0$-pair and the $(K\pi)$-pair vertices are not determined in the ESC model and therefore we take such a prescription that two effective two-body potentials $V_{(\pi\pi)_0}^{(\mathrm{eff.2B})}(r)$ and $V_{(K\pi)}^{(\mathrm{eff.2B})}(r)$ do not contribute to the two-nucleon induced non-mesonic decay rate calculations. Accordingly, the calculations are done with the effective two-body potential as

$$V^{(\mathrm{eff.2B})}(r) \;=\; V_{(\pi\sigma)}^{(\mathrm{eff.2B})}(r) + V_{(\pi\omega)}^{(\mathrm{eff.2B})}(r) + V_{(\sigma\sigma)}^{(\mathrm{eff.2B})}(r) + V_{FM(\pi\pi)}^{(\mathrm{eff.2B})}(r), \tag{85}$$

for which four different sets of meson-pair coupling constants are used for the $(\pi\sigma)$ and $(\pi\omega)$ pairs, and the $(\sigma\sigma)$ pair and the Fujita–Miyazawa $(\pi\pi)$ pair as listed in Table 1 are used.

For clarification, we use the following symbols for the sum of potentials:

$$V\mathrm{E15} \;:\; \left\{ V_{(\pi\sigma)}^{(\mathrm{eff.2B})} + V_{(\pi\omega)}^{(\mathrm{eff.2B})} \right\},\ \text{adopting E15 coupling constants}$$

$$V\mathrm{E10} \;:\; \left\{ V_{(\pi\sigma)}^{(\mathrm{eff.2B})} + V_{(\pi\omega)}^{(\mathrm{eff.2B})} \right\},\ \text{adopting E10 coupling constants}$$

$$V\mathrm{E16} \;:\; \left\{ V_{(\pi\sigma)}^{(\mathrm{eff.2B})} + V_{(\pi\omega)}^{(\mathrm{eff.2B})} \right\},\ \text{adopting E16 coupling constants}$$

$$V\mathrm{E19} \;:\; \left\{ V_{(\pi\sigma)}^{(\mathrm{eff.2B})} + V_{(\pi\omega)}^{(\mathrm{eff.2B})} \right\},\ \text{adopting E19 coupling constants.}$$

As for the $(\sigma\sigma)$-pair coupling constant, three values $g_{(\sigma\sigma)}(a)$, $g_{(\sigma\sigma)}(b)$, and $g_{(\sigma\sigma)}(c)$ listed in Table 1 are tried. The reasons for adopting $g_{(\sigma\sigma)} < 0$ are as follows. (i) The strong interaction $V_{(\sigma\sigma)}^{(\mathrm{eff.2B})}(NN\text{–}NN)$ makes an attractive contribution to the nuclear matter binding energy and a nice energy value is obtained for $g_{(\sigma\sigma)}/4\pi = -(0.3\text{–}0.4)$. (ii) It is assumed that the NN- and YN-scattering data can be accounted for with no problem with inclusion of the coupling constant $g_{(\sigma\sigma)}/4\pi = -0.3$ together with the meson-pair ones and the baryon–baryon–meson ones of the ESC16 model [26,27,33]. (iii) A potential due to the $(\sigma\sigma)$-pair exchange is found to have a favorable effect on the U_Ξ potential. (iv) Another discussion exists. First the σ^3-Hamiltonian is defined as

$$\mathcal{H}_{3\sigma} = \frac{1}{3!}\, g_{\sigma\sigma\sigma}\, m_\sigma\, \phi_\sigma^3. \tag{86}$$

Evaluating the diagrams depicted in Fig. 3, we obtain

Table 2. Calculated non-mesonic decay rates $\Gamma_{nm}^{(\mathrm{eff.2B})}$ of ${}^{5}_{\Lambda}$He, ${}^{11}_{\Lambda}$B, and ${}^{12}_{\Lambda}$C and their dependence on the four cases of effective two-body potentials used: (1) VE15 + $V_{(\sigma\sigma)}$ + $V_{FM(\pi\pi)}$, (2) VE10 + $V_{(\sigma\sigma)}$ + $V_{FM(\pi\pi)}$, (3) VE16 + $V_{(\sigma\sigma)}$ + $V_{FM(\pi\pi)}$, and (4) VE19 + $V_{(\sigma\sigma)}$ + $V_{FM(\pi\pi)}$. For the $V_{(\sigma\sigma)}$ potential, the coupling constant is fixed to $g_{(\sigma\sigma)}/4\pi = -0.300$. For p-shell hypernuclei, calculations are shown for the wave functions with the configuration-mixed shell model + Λ particle. The experimental $\Gamma_{2N}^{\mathrm{exp}}$ data are also listed. Decay rates are given in units of free Λ decay rate Γ_Λ.

	(1)	(2)	(3)	(4)	Exp.
${}^{5}_{\Lambda}$He($1/2^+$)	0.083	0.068	0.073	0.093	0.078 ± 0.034 [13]
${}^{11}_{\Lambda}$B($5/2^+$)	0.176	0.150	0.160	0.194	0.169 ± 0.077 [13]
${}^{12}_{\Lambda}$C(1^-)	0.197	0.167	0.178	0.219	0.178 ± 0.076 [13]
					0.27 ± 0.13 [8,9]

$$< N'\,\sigma' \mid M \mid N\,\sigma\ > = g_{NN\sigma} g_{\sigma\sigma\sigma}\, m_\sigma\, [\,\bar{u}(p')\,u(p)]\frac{1}{k^2 - m_\sigma^2 + i\epsilon}$$

$$= 2\,\frac{g_{(\sigma\sigma)}}{m_\pi}\,[\bar{u}(p')\,u(p)], \tag{87}$$

which gives, using the low-energy approximation,

$$g_{(\sigma\sigma)} \simeq -\,g_{NN\sigma}\, g_{\sigma\sigma\sigma}\,\frac{m_\pi}{2m_\sigma}. \tag{88}$$

Kleinert gives a formula [34], f_π being 93 MeV and $m_\sigma = 600.0$ MeV,

$$g_{\sigma\sigma\sigma} = 3\,\frac{m_\sigma}{f_\pi}\left(1 - \frac{m_\pi^2}{m_\sigma^2}\right) \approx 18.3. \tag{89}$$

Then we get $g_{(\sigma\sigma)}/4\pi \approx -1.06$, which shows $g_{(\sigma\sigma)} < 0$.

On the other hand, comparing Eq. (86) with the MFT described in Glendenning [35] with the interaction Lagrangian $\mathcal{L}_{3\sigma} = -(b/3)\,m_{\mathrm{N}} g_{NN\sigma}^3 \phi_\sigma^3$ gives

$$g_{\sigma\sigma\sigma} = 2\frac{m_{\mathrm{N}}}{m_\sigma}\,b\,g_{NN\sigma}^3. \tag{90}$$

Here, $b = (0.5\text{–}1.5) \times 10^{-2}$ is used. Then we find $g_{\sigma\sigma\sigma} \approx (3.91\text{–}11.73)$ and get $g_{(\sigma\sigma)}/4\pi = -(0.23\text{–}0.68)$, which also shows $g_{(\sigma\sigma)} < 0$.

The decay rates $\Gamma_p^{(\mathrm{eff.2B})}$, $\Gamma_n^{(\mathrm{eff.2B})}$, and $\Gamma_{nm}^{(\mathrm{eff.2B})}$ have strong dependence on the adopted coupling constants that have uncertainties among various versions of the ESC and GESC models. In Table 2, calculated non-mesonic decay rates $\Gamma_{nm}^{(\mathrm{eff.2B})}$ of ${}^{5}_{\Lambda}$He, ${}^{11}_{\Lambda}$B, and ${}^{12}_{\Lambda}$C are shown focusing on their dependence on the four types of MPE potentials of the sum of $(\pi\sigma)$ and $(\pi\omega)$ exchanges abbreviated as VE15, VE10, VE16, and VE19, when $V_{(\sigma\sigma)}$ and $V_{FM(\pi\pi)}$ are fixed. The total effective two-body potentials used are

(1) VE15 + $V_{(\sigma\sigma)}$ + $V_{FM(\pi\pi)}$,
(2) VE10 + $V_{(\sigma\sigma)}$ + $V_{FM(\pi\pi)}$,
(3) VE16 + $V_{(\sigma\sigma)}$ + $V_{FM(\pi\pi)}$, and
(4) VE19 + $V_{(\sigma\sigma)}$ + $V_{FM(\pi\pi)}$.

For $V_{(\sigma\sigma)}$, the meson-pair coupling constant $g_{(\sigma\sigma)}/4\pi = -0.300$ is adopted here.

It is known for each of the three hypernuclear decays that the calculated $\Gamma_{nm}^{(\mathrm{eff.2B})}$ have some variances among the four cases of potentials (1)–(4). VE19 and VE15 make large contributions to the decay rates, while VE10 and VE16 make moderate ones. In calculations, we adopt two types of shell model wave functions, the Cohen–Kurath-type configuration-mixed shell model

Table 3. Contributions from various combinations of potentials to $\Gamma_{nm}^{(\mathrm{eff.2B})}$ are shown for ${}^{5}_{\Lambda}$He. *V*E19 signifies the potentials of $V_{(\pi\sigma)} + V_{(\pi\omega)}$ with E19 coupling constants and $V_{(\sigma\sigma)}$ is the case of using the coupling constant $g_{(\sigma\sigma)}/4\pi = -0.300$. $V_{FM(\pi\pi)}$ is fixed uniquely. $\Gamma_{2N}^{\mathrm{exp}}$ is shown for comparison. Decay rates are given in units of free Λ decay rate Γ_Λ.

	$\Gamma_{nm}^{(\mathrm{eff.2B})}$	$\Gamma_{2N}^{\mathrm{exp}}$
*V*E19	0.035	
$V_{(\sigma\sigma)}$	0.054	
V_{FM}	0.005	
$V_{(\sigma\sigma)} + V_{FM}$	0.063	
*V*E19 + V_{FM}	0.017	
*V*E19 + $V_{(\sigma\sigma)}$	0.107	
*V*E19 + $V_{(\sigma\sigma)} + V_{FM}$	0.093	
		0.078 ± 0.034 [13]

and the simple HO shell model, for the core-nucleus part of *p*-shell hypernuclei and the daughter nuclei, but the differences in $\Gamma_{nm}^{(\mathrm{eff.2B})}$ are small between the two cases.

In Table 3, we display the contributions of various combinations of effective two-body potentials, $V_{(\pi\sigma)}$, $V_{(\pi\omega)}$, $V_{(\sigma\sigma)}$, and $V_{FM(\pi\pi)}$, to the decay rate $\Gamma_{nm}^{(\mathrm{eff.2B})}$ for ${}^{5}_{\Lambda}$He as an example. Here we show the case where the meson-pair coupling constants of $V_{(\pi\sigma)}$ and $V_{(\pi\omega)}$ are chosen to be the set of E19, that of $V_{(\sigma\sigma)}$ is $g_{(\sigma\sigma)}/4\pi = -0.300$, and $V_{FM(\pi\pi)}$ is unique. The $V_{(\sigma\sigma)}$ potential yields a large contribution to the decay rate. One can see that the contribution of $V_{FM(\pi\pi)}$ alone is small compared with *V*E19 and/or $V_{(\sigma\sigma)}$. However, $V_{FM(\pi\pi)}$ works destructively against *V*E19 as seen in the decay rate in the case of *V*E19 + V_{FM}, while in contrast $V_{FM(\pi\pi)}$ works additively to $V_{(\sigma\sigma)}$ as seen in the case of $V_{(\sigma\sigma)} + V_{FM}$. The total *V*E19 + $V_{(\sigma\sigma)} + V_{FM}$ gives $\Gamma_{nm}^{(\mathrm{eff.2B})}$ as a comparable magnitude to $\Gamma_{2N}^{\mathrm{exp}}$ in the present case. Thus one knows that each of *V*E19, $V_{(\sigma\sigma)}$, and V_{FM} has a proper and important role in producing the non-mesonic decay rate.

Table 4 shows the calculated non-mesonic decay rates $\Gamma_{p}^{(\mathrm{eff.2B})}$, $\Gamma_{n}^{(\mathrm{eff.2B})}$, and $\Gamma_{nm}^{(\mathrm{eff.2B})}$ of hypernuclei ${}^{5}_{\Lambda}$He, ${}^{11}_{\Lambda}$B, and ${}^{12}_{\Lambda}$C and their dependence on the $V_{(\sigma\sigma)}$ potential used in the effective two-body potentials of $V_{(\pi\sigma)} + V_{(\pi\omega)} + V_{(\sigma\sigma)} + V_{FM(\pi\pi)}$. Here the case is shown that the E19 potential of $V_{(\pi\sigma)} + V_{(\pi\omega)}$ is chosen and $V_{(\sigma\sigma)}$ is varied by adopting the three different coupling constants $g_{(\sigma\sigma)}/4\pi = -0.150$, -0.300, and -0.325. $V_{FM(\pi\pi)}$ is unique.

One sees in Table 4 that the calculated decay rates $\Gamma_{p}^{(\mathrm{eff.2B})}$, $\Gamma_{n}^{(\mathrm{eff.2B})}$, and $\Gamma_{nm}^{(\mathrm{eff.2B})}$ have a strong dependence on the $V_{(\sigma\sigma)}$ potential with the adopted coupling constant $g_{(\sigma\sigma)}$. This feature is common to ${}^{5}_{\Lambda}$He, ${}^{11}_{\Lambda}$B, and ${}^{12}_{\Lambda}$C decays. These tendencies are also observed in other combinations of potentials even when we replace *V*E19 with *V*E15, *V*E10, or *V*E16, respectively. Such features clearly show the importance of the $V_{(\sigma\sigma)}$ potential in producing the enhanced $\Gamma_{nm}^{(\mathrm{eff.2B})}$. Note, however, that $V_{(\sigma\sigma)}$ is exclusively a spin–isospin-independent central force while $V_{(\pi\sigma)}$, $V_{(\pi\omega)}$, and $V_{FM(\pi\pi)}$ have spin–isospin-dependent central and tensor forces. Therefore, each of the MPE $V_{(\pi\sigma)}$, $V_{(\pi\omega)}$, $V_{(\sigma\sigma)}$, and $V_{FM(\pi\pi)}$ has its proper role of yielding $\Gamma_{nm}^{(\mathrm{eff.2B})}$.

In view of the theory–experiment comparison in Tables 2 and 4, we conclude that we can understand the two-nucleon induced decay rates $\Gamma_{2N}^{\mathrm{exp}}$ of ${}^{5}_{\Lambda}$He, ${}^{11}_{\Lambda}$B, and ${}^{12}_{\Lambda}$C with the effective two-body potential model, when we make an allowance for choosing $V_{(\sigma\sigma)}$ with $g_{(\sigma\sigma)}/4\pi \simeq -(0.300\text{–}0.325)$ and selecting, for instance, *V*E19 or *V*E16 for $V_{(\pi\sigma)} + V_{(\pi\omega)}$ potential and $V_{FM(\pi\pi)}$.

Table 4. Calculated non-mesonic decay rates, $\Gamma_p^{(\mathrm{eff.2B})}$, $\Gamma_n^{(\mathrm{eff.2B})}$, and $\Gamma_{nm}^{(\mathrm{eff.2B})}$, of ${}^{5}_{\Lambda}$He, ${}^{11}_{\Lambda}$B, and ${}^{12}_{\Lambda}$C and their dependence on the $V_{(\sigma\sigma)}$ potential used in $V_{(\pi\sigma)} + V_{(\pi\omega)} + V_{(\sigma\sigma)} + V_{FM(\pi\pi)}$. In the choice of a combination "VE19 + $V_{(\sigma\sigma)} + V_{FM}$", $V_{(\sigma\sigma)}$ is varied by adopting three different coupling constants $g_{(\sigma\sigma)}$ and $V_{FM(\pi\pi)}$ is uniquely fixed. For p-shell hypernuclei, calculations are shown for the wave functions with the configuration-mixed shell model + Λ particle. Experimental data $\Gamma_{2N}^{\mathrm{exp}}$ and $\Gamma_{NM}^{\mathrm{exp}}$(total) are shown for comparison. Decay rates are given in units of free Λ decay rate Γ_Λ.

	VE19 + $V_{(\sigma\sigma)} + V_{FM}$			
	$g_{(\sigma\sigma)}/4\pi$ $=-0.150$	$g_{(\sigma\sigma)}/4\pi$ $=-0.300$	$g_{(\sigma\sigma)}/4\pi$ $=-0.325$	Exp.
${}^{5}_{\Lambda}$He $(1/2^+)$				
$\Gamma_p^{(\mathrm{eff.2B})}$	0.035	0.073	0.081	
$\Gamma_n^{(\mathrm{eff.2B})}$	0.007	0.020	0.023	
$\Gamma_{nm}^{(\mathrm{eff.2B})}$	0.042	0.093	0.104	$\Gamma_{2N}^{\mathrm{exp}} = 0.078 \pm 0.034$ [13] $\Gamma_{NM}^{\mathrm{exp}} = 0.424 \pm 0.024$ [36,37]
${}^{11}_{\Lambda}$B $(5/2^+)$				
$\Gamma_p^{(\mathrm{eff.2B})}$	0.066	0.144	0.161	
$\Gamma_n^{(\mathrm{eff.2B})}$	0.016	0.051	0.058	
$\Gamma_{nm}^{(\mathrm{eff.2B})}$	0.082	0.194	0.219	$\Gamma_{2N}^{\mathrm{exp}} = 0.169 \pm 0.077$ [13] $\Gamma_{NM}^{\mathrm{exp}} = 0.861 \pm 0.063^{+0.073}_{-0.073}$ [38]
${}^{12}_{\Lambda}$C (1^-)				
$\Gamma_p^{(\mathrm{eff.2B})}$	0.078	0.168	0.188	
$\Gamma_n^{(\mathrm{eff.2B})}$	0.016	0.050	0.058	
$\Gamma_{nm}^{(\mathrm{eff.2B})}$	0.094	0.219	0.246	$\Gamma_{2N}^{\mathrm{exp}} = 0.178 \pm 0.076$ [13] 0.27 ± 0.13 [8,9] $\Gamma_{NM}^{\mathrm{exp}} = 0.940 \pm 0.035$ [36] $0.828 \pm 0.056^{+0.066}_{-0.066}$ [38]

Here we remember the following facts. In the course of the derivation of the effective two-body potentials, the weak three-body interactions with particular MPE such as $(\pi\sigma)$-, $(\pi\omega)$-, and $(\sigma\sigma)$-pair exchanges and the Fujita–Miyazawa $(\pi\pi)$ exchange are found to contribute appreciably to the effective potentials. On the other hand, we know that some other possibly important three-body interactions are lost as a consequence of the present approximation procedure. Further, the adopted meson-pair coupling constants still have some uncertainties. Thus our calculated $\Gamma_{nm}^{(\mathrm{eff.2B})}$ should be regarded as the "order of magnitude" of the two-nucleon induced Γ_{2N} at the present stage.

7. Summary and remarks

With the hope of determining the role of the three-body $\Lambda NN \to NNN$ interaction in the two-nucleon induced non-mesonic decay rates Γ_{2N} of light and p-shell hypernuclei, we evaluate the effective two-body decay rates with use of the effective two-body potential $V^{(\mathrm{eff.2B})}(\Lambda N$–$NN)$ deduced from the three-body $\Lambda NN \to NNN$ interaction.

First of all, the three-body weak $\Lambda NN \to NNN$ interactions are constructed in a model of meson-pair exchange among Λ and two nucleons, where the weak vertex is considered either at the ΛN–meson vertex or at the ΛN–(meson-pair) one. The effective two-body potential $V^{(\mathrm{eff.2B})}(\Lambda N$–$NN)$ is deduced from the three-body interactions by integrating out the

particle-"3" coordinate, spin, and isospin variables following the LNR approximation method. The limited number of weak three-body interactions of $V^{\rm W3B}_{(m_1m_2)}(\Lambda NN - NNN)$ with particular MPE contribute to the effective two-body potentials through reduction and approximation. The obtained effective potential $V^{\rm (eff.2B)}(\Lambda N\text{–}NN)$ consists of $V_{(\pi\pi)_0}$, $V_{(\pi\sigma)}$, $V_{(\pi\omega)}$, $V_{(K\pi)}$, $V_{(\sigma\sigma)}$, and $V_{FM(\pi\pi)}$.

The strong NN-(meson-pair) coupling constants are taken from various versions of the ESC and GESC models, while the weak ΛN-(meson-pair) ones for their parity-conserving parts are evaluated in this work from the weak Λ–n mixing model by Dalitz–Von Hippel and the mixing angle ε, which gives the relation $g^{(w)}_{\Lambda N\text{(meson-pair)}} = \varepsilon\, g^{(s)}_{NN\text{(meson-pair)}}$. Here ε is obtained through evaluation of the $\Lambda \to n$ weak transition matrix element by employing the quark-model wave functions for Λ and the neutron and the quark–quark interaction $V_{QQ}(r)$ due to the internal meson (pion) exchange.

In the ESC model, however, the strong meson-pair coupling constant $g_{(\pi\pi)_0}$ has not been determined so far and is set to 0, and also no attempt has been made to fix $g_{(K\pi)}$ yet. Therefore, we adopt the four types of the effective two-body potentials as $V_{(\pi\sigma)}$, $V_{(\pi\omega)}$, $V_{(\sigma\sigma)}$, and $V_{FM(\pi\pi)}$ for the weak decay rate calculations in this paper.

The potential character is different between the $V_{(\pi\sigma)}$, $V_{(\pi\omega)}$, $V_{(\sigma\sigma)}$, and $V_{FM(\pi\pi)}$ potentials. For the parity-conserving part, $V_{(\sigma\sigma)}$ is a spin–isospin-independent central potential, while $V_{(\pi\sigma)}$, $V_{(\pi\omega)}$, and $V_{FM(\pi\pi)}$ have spin–isospin-dependent central and tensor force components. The tensor forces of $V_{(\pi\sigma)}$ and $V_{(\pi\omega)}$ work in the same sign, but they work oppositely to that of $V_{FM(\pi\pi)}$.

$V^{\rm (eff.2B)}(\Lambda N\text{–}NN)$ is applied to evaluate the effective two-body decay rates $\Gamma^{\rm (eff.2B)}_{nm}$ of ${}^{5}_{\Lambda}$He, ${}^{11}_{\Lambda}$B, and ${}^{12}_{\Lambda}$C. The calculated $\Gamma^{\rm (eff.2B)}_{nm}$ strongly depend on the adopted strong and weak meson-pair coupling constants, which have some uncertainties in the ESC and GESC models and on the mixing angle ε. The fixed $\varepsilon = -0.758 \times 10^{-7}$ is currently used.

Four sets of meson-pair coupling constants for the $(\pi\sigma)$ and $(\pi\omega)$-exchange potentials are examined, $g_{(\sigma\sigma)}$ in $V_{(\sigma\sigma)}$ is treated as a free parameter, and the coupling constants of the Fujita–Miyazawa-type potential are fixed to the original ones.

When we choose the coupling constants E19 for the $(\pi\sigma)$ and $(\pi\omega)$ pairs and $g_{(\sigma\sigma)}/4\pi = -(0.300\text{–}0.325)$ for the $(\sigma\sigma)$-pair coupling, for which we denote the total potential as VE19 $+ V_{(\sigma\sigma)} + V_{FM}$, the calculated $\Gamma^{\rm (eff.2B)}_{nm}$ are $(0.093\text{–}0.104)\Gamma_\Lambda$ for ${}^{5}_{\Lambda}$He, $(0.194\text{–}0.219)\Gamma_\Lambda$ for ${}^{11}_{\Lambda}$B, and $(0.219\text{–}0.246)\Gamma_\Lambda$ for ${}^{12}_{\Lambda}$C. The calculated $\Gamma^{\rm (eff.2B)}_{nm}$ are compatible with the available two-nucleon induced $\Gamma^{\rm exp}_{2N}$ of the FINUDA or KEK E462-E508 data within the error bars for these hypernuclear decays. Similar but slightly smaller decay rates are obtained for the potential VE16 $+ V_{(\sigma\sigma)} + V_{FM}$. It is also found that the adopted potentials $V_{(\pi\sigma)}$, $V_{(\pi\omega)}$, $V_{(\sigma\sigma)}$, and $V_{FM(\pi\pi)}$ have their own proper roles in producing $\Gamma^{\rm (eff.2B)}_{nm}$.

Thus we may say that it is possible for us to understand the two-nucleon induced decay rates $\Gamma^{\rm exp}_{2N}$ for ${}^{5}_{\Lambda}$He, ${}^{11}_{\Lambda}$B, and ${}^{12}_{\Lambda}$C in the effective two-body potentials deduced from the MPE three-body ΛNN–NNN interactions if we properly choose the meson-pair coupling constants for $(\pi\sigma)$, $(\pi\omega)$, $(\sigma\sigma)$, and Fujita–Miyazawa $(\pi\pi)$ exchanges.

We, however, bear in mind the following. First, the three-body $\Lambda NN \to NNN$ interactions in our MPE model are not fully taken into account in obtaining the effective two-body $\Lambda N \to NN$ potentials, because a number of possibly important MPE three-body interactions are lost in the deduction process. Second, the roles of the potentials of $V_{(\pi\pi)_0}$ and $V_{(K\pi)}$ are not studied in this paper; this is left as an open problem because at present we do not have firm knowledge of those

meson-pair coupling constants. Third, the NN-(meson-pair) coupling constants, especially the $NN(\sigma\sigma)$ one, are not well constrained and have uncertainties. Fourth, the decay dynamics in the effective two-body potential model is decisively different from that in the three-body $\Lambda NN \to NNN$ decays, especially in the energy share for the final decaying nucleons. We cannot predict the decay rate ratio such as $\Gamma_{np} : \Gamma_{pp} : \Gamma_{nn}$ in the present model, but this problem should be the next subject to study.

Therefore, we consider at present that the calculated $\Gamma_{nm}^{(\mathrm{eff.2B})}$ for light and p-shell hypernuclei should give a limited estimate of the two-nucleon induced decay rate Γ_{2N}. A more advanced method of handling the three-body $\Lambda NN \to NNN$ interactions would elucidate the three-body weak non-mesonic decay mechanism.

Acknowledgment

We are grateful to Y. Yamamoto and E. Hiyama for their continuing interest in this subject. K.I. would like to express his sincere thanks to K. Nakazawa for the warm hospitality at Gifu University extended to him over long years.

Appendix A. Weak effective two-body interactions $\tilde{V}^W(\boldsymbol{k}, -\boldsymbol{k}, \boldsymbol{q})$

The interaction $\tilde{V}^W(\boldsymbol{k}, -\boldsymbol{k}, \boldsymbol{q})$ is the form given after applying $(1/4)Tr$-operators for $\boldsymbol{\sigma}_3$ and $\boldsymbol{\tau}_3$ and averaging $\boldsymbol{q}_3^2$ and $\boldsymbol{q}_3$ for the full form of $V^{\mathrm{W3B}}(\boldsymbol{k}, -\boldsymbol{k}, 0, \boldsymbol{q}, -\boldsymbol{q}, \boldsymbol{q}_3, \boldsymbol{\sigma}_1, \boldsymbol{\sigma}_2, \boldsymbol{\sigma}_3, \boldsymbol{\tau}_1, \boldsymbol{\tau}_2, \boldsymbol{\tau}_3)$. The relations $< \boldsymbol{q}_3^2 >= (3/5)\, k_F^2$ and $< \boldsymbol{q}_3 >= 0$ are used. The weak effective interactions in momentum space are given for $(\pi\pi)_0$, $(\pi\sigma)$, $(\pi\omega)$, $(K\pi)$, $(\sigma\sigma)$, and Fujita–Miyazawa $(\pi\pi)$ exchanges. It is noted that ρ_{NM} is not attached here.

1. $J^{PC} = 0^{++}$: $(\pi\pi)_0$-pair exchange

$$\begin{aligned}\tilde{V}^W_{(\pi\pi)_0}(\boldsymbol{k}, -\boldsymbol{k}, \boldsymbol{q}) = {} & \frac{g_{(\pi\pi)_0}}{m_\pi}\, g_\pi^w\, \frac{f_\pi}{m_\pi}\, 2M_N \\ & \times \left\{ \lambda\, \frac{1}{4\bar{M} M_N} (\boldsymbol{\sigma}_1 \cdot \boldsymbol{k})(\boldsymbol{\sigma}_2 \cdot \boldsymbol{k}) \; - \frac{1}{2M_N} (\boldsymbol{\sigma}_2 \cdot \boldsymbol{k}) \right. \\ & \left. \times \left[1 + \frac{\boldsymbol{k}^2}{8\bar{M}^2} - \frac{i(\boldsymbol{k} \times \boldsymbol{q}) \cdot \boldsymbol{\sigma}_1}{4\bar{M}^2} \right] \right\} \cdot (\boldsymbol{\tau}_1 \cdot \boldsymbol{\tau}_2)\; \frac{1}{\boldsymbol{k}^2 + m_\pi^2}\, \frac{1}{\boldsymbol{k}^2 + m_\pi^2} \end{aligned} \tag{A1}$$

2. $J^{PC} = 1^{++}$: $(\pi\sigma)$-pair exchange

$$\begin{aligned}\tilde{V}^W_{(\pi\sigma)}(\boldsymbol{k}, -\boldsymbol{k}, \boldsymbol{q}) = {} & \frac{g_{(\pi\sigma)} g_\sigma}{m_\pi^2}\, g_\pi^w\, 2M_N \\ & \times \left\{ \lambda\, \frac{(\boldsymbol{\sigma}_1 \cdot \boldsymbol{k})}{2\bar{M}} \left[\frac{(\boldsymbol{\sigma}_2 \cdot \boldsymbol{k})}{2M_N} + \frac{(\boldsymbol{\sigma}_2 \cdot \boldsymbol{q})}{M_N}\, \frac{(\boldsymbol{q} \cdot \boldsymbol{k})}{2\bar{M} M_N} \right] \right. \\ & \left. - \left[\frac{(\boldsymbol{\sigma}_2 \cdot \boldsymbol{k})}{2M_N} + \frac{(\boldsymbol{\sigma}_2 \cdot \boldsymbol{q})}{M_N}\, \frac{(\boldsymbol{q} \cdot \boldsymbol{k})}{2\bar{M} M_N} \right] \right.\end{aligned}$$

$$
\begin{aligned}
&- \frac{(\boldsymbol{\sigma}_2\cdot\boldsymbol{k})}{2M_N}\left[\frac{\boldsymbol{k}^2}{8\bar{M}^2} - \frac{i(\boldsymbol{k}\times\boldsymbol{q})\cdot\boldsymbol{\sigma}_1}{4\bar{M}^2}\right]\Bigg\}\cdot\,(\boldsymbol{\tau}_1\cdot\boldsymbol{\tau}_2)\,\frac{1}{\boldsymbol{k}^2+m_\pi^2}\,\frac{1}{m_\sigma^2}\\
&+\frac{G_F m_\pi^2}{m_\pi^2}\,\frac{f_\pi}{m_\pi}\,g_\sigma\,(2M_N)^2\\
&\times\Bigg\{A^{pc}_{(\pi\sigma)}\left[\frac{(\boldsymbol{\sigma}_1\cdot\boldsymbol{k})}{2M_N}+\frac{(\boldsymbol{\sigma}_1\cdot\boldsymbol{q})}{M_N}\,\frac{(\boldsymbol{q}\cdot\boldsymbol{k})}{2\bar{M}M_N}\right]\frac{(\boldsymbol{\sigma}_2\cdot\boldsymbol{k})}{2M_N}\\
&+B^{pv}_{(\pi\sigma)}\left[\frac{(\boldsymbol{q}\cdot\boldsymbol{k})}{2\bar{M}M_N}+\frac{(\boldsymbol{q}\cdot\boldsymbol{k})}{2{M_N}^2}\right]\frac{(\boldsymbol{\sigma}_2\cdot\boldsymbol{k})}{2M_N}\Bigg\}\cdot\,(\boldsymbol{\tau}_1\cdot\boldsymbol{\tau}_2)\,\frac{1}{\boldsymbol{k}^2+m_\pi^2}\,\frac{1}{m_\sigma^2}
\end{aligned}
\tag{A2}
$$

3. $J^{PC}=1^{+-}$: $(\pi\omega)$-pair exchange

$$
\begin{aligned}
\tilde{V}^W_{(\pi\omega)}(\boldsymbol{k},-\boldsymbol{k},\,\boldsymbol{q}) = &-\frac{g_{(\pi\omega)}g_\omega}{m_\pi^2}\,g_\pi^w\,2M_N\\
&\times\Bigg\{\lambda\,\frac{1}{4\bar{M}M_N}(\boldsymbol{\sigma}_1\cdot\boldsymbol{k})(\boldsymbol{\sigma}_2\cdot\boldsymbol{k})\left[1+\frac{1}{2M_N^2}\frac{3}{5}k_F^2\right]\\
&-\frac{1}{2M_N}(\boldsymbol{\sigma}_2\cdot\boldsymbol{k})\left[1+\frac{1}{2M_N^2}\frac{3}{5}k_F^2+\frac{\boldsymbol{k}^2}{8\bar{M}M_N}-\frac{i(\boldsymbol{k}\times\boldsymbol{q})\cdot\boldsymbol{\sigma}_1}{4\bar{M}M_N}\right]\Bigg\}\\
&\cdot\,(\boldsymbol{\tau}_1\cdot\boldsymbol{\tau}_2)\frac{1}{\boldsymbol{k}^2+m_\pi^2}\,\frac{1}{m_\omega^2}\\
&-\frac{G_F m_\pi^2}{m_\pi^2}\,\frac{f_\pi}{m_\pi}\,g_\omega\,2M_N\,2\bar{M}\\
&\times\Bigg\{A^{pc}_{(\pi\omega)}\,\frac{1}{4\bar{M}M_N}(\boldsymbol{\sigma}_1\cdot\boldsymbol{k})(\boldsymbol{\sigma}_2\cdot\boldsymbol{k})\left[1-\frac{f_\omega}{g_\omega}\,\frac{1}{2M_N^2}\frac{3}{5}k_F^2\right]\\
&-B^{pv}_{(\pi\omega)}\,\frac{1}{2M_N}(\boldsymbol{\sigma}_2\cdot\boldsymbol{k})\left[\frac{\boldsymbol{k}^2}{4\bar{M}^2}-\frac{i(\boldsymbol{k}\times\boldsymbol{q})\cdot\sigma_1}{2\bar{M}^2}\right]\Bigg\}\\
&\cdot\,(\boldsymbol{\tau}_1\cdot\boldsymbol{\tau}_2)\,\frac{1}{\boldsymbol{k}^2+m_\pi^2}\,\frac{1}{m_\omega^2}
\end{aligned}
\tag{A3}
$$

4. $J^P=0^+$: $(K\pi)$-pair exchange

$$
\begin{aligned}
\tilde{V}^W_{(K\pi)}(\boldsymbol{k},-\boldsymbol{k},\,\boldsymbol{q}) = &-\frac{G_F m_\pi^2}{m_\pi}\,g_{(K\pi)}\,\frac{f_\pi}{m_\pi}\,2M_N\\
&\times\left[\frac{1}{2}\,C_K^{pv}+D_K^{pv}\right]\frac{(\boldsymbol{\sigma}_2\cdot\boldsymbol{k})}{2M_N}\left[1+\frac{\boldsymbol{k}^2}{8\bar{M}^2}-\frac{i(\boldsymbol{k}\times\boldsymbol{q})\cdot\boldsymbol{\sigma}_1}{4\bar{M}^2}\right]\\
&\cdot\,(\boldsymbol{\tau}_1\cdot\boldsymbol{\tau}_2)\frac{1}{m_K^2}\,\frac{1}{\boldsymbol{k}^2+m_\pi^2}\\
&+\frac{G_F m_\pi^2}{m_\pi}\,g_{\Lambda NK}\,\frac{f_\pi}{m_\pi}\,2M_N\\
&\times\frac{1}{2}\,C^{pc}_{(K\pi)}\,\frac{(\boldsymbol{\sigma}_1\cdot\boldsymbol{k})(\boldsymbol{\sigma}_2\cdot\boldsymbol{k})}{4\bar{M}M_N}\cdot\,(\boldsymbol{\tau}_1\cdot\boldsymbol{\tau}_2)\frac{1}{\boldsymbol{k}^2+m_K^2}\,\frac{1}{\boldsymbol{k}^2+m_\pi^2}
\end{aligned}
\tag{A4}
$$

5. $J^{PC} = 0^{++}$: $(\sigma\sigma)$-pair exchange

$$\begin{aligned}
\tilde{V}^{W}_{(\sigma\sigma)}(\boldsymbol{k}, -\boldsymbol{k}, \boldsymbol{q}) = {} & G_F m_\pi^2 \frac{g_{(\sigma\sigma)}}{m_\pi} g_\sigma \\
& \times \left\{ A^{pc}_{\sigma} \left[1 + \frac{\boldsymbol{k}^2}{4\bar{M} M_N} - \frac{i(\boldsymbol{k}\times\boldsymbol{q})\cdot\boldsymbol{\sigma}_1 + i(\boldsymbol{k}\times\boldsymbol{q})\cdot\boldsymbol{\sigma}_2}{4\bar{M} M_N} \right] \right. \\
& \left. - B^{pv}_{\sigma} \frac{(\boldsymbol{\sigma}_1\cdot\boldsymbol{k})}{2M_N} \left[1 + \frac{\boldsymbol{k}^2}{8{M_N}^2} - \frac{i(\boldsymbol{k}\times\boldsymbol{q})\cdot\boldsymbol{\sigma}_2}{4{M_N}^2} \right] \right\} \\
& \cdot \left[\frac{1}{\boldsymbol{k}^2 + m_\sigma^2} \frac{1}{\boldsymbol{k}^2 + m_\sigma^2} + \frac{1}{\boldsymbol{k}^2 + m_\sigma^2} \frac{1}{m_\sigma^2} \right] \\
& + G_F m_\pi^2 \frac{g_\sigma^2}{m_\pi} \\
& \times \left\{ A^{pc}_{\sigma\sigma} \left[1 + \frac{\boldsymbol{k}^2}{4\bar{M} M_N} - \frac{i(\boldsymbol{k}\times\boldsymbol{q})\cdot\boldsymbol{\sigma}_1 + i(\boldsymbol{k}\times\boldsymbol{q})\cdot\boldsymbol{\sigma}_2}{4\bar{M} M_N} \right] \right. \\
& \left. - B^{pv}_{\sigma\sigma} \frac{(\boldsymbol{\sigma}_1\cdot\boldsymbol{k})}{2M_N} \left[1 + \frac{\boldsymbol{k}^2}{8{M_N}^2} - \frac{i(\boldsymbol{k}\times\boldsymbol{q})\cdot\boldsymbol{\sigma}_2}{4{M_N}^2} \right] \right\} \\
& \cdot \frac{1}{\boldsymbol{k}^2 + m_\sigma^2} \frac{1}{m_\sigma^2}
\end{aligned} \tag{A5}$$

6. Fujita–Miyazawa $(\pi\pi)$-pair exchange

$$\begin{aligned}
\tilde{V}^{W}_{FM(\pi\pi)}(\boldsymbol{k}, -\boldsymbol{k}, \boldsymbol{q}) = {} & -g^w_\pi \frac{f_\pi}{m_\pi} 2M_N \\
& \times \left\{ \lambda \frac{1}{4\bar{M} M_N} (\boldsymbol{\sigma}_1\cdot\boldsymbol{k})(\boldsymbol{\sigma}_2\cdot\boldsymbol{k}) \left[(A+B)\frac{\boldsymbol{k}^2}{m_\pi^3} + D\frac{1}{m_\pi} \right] \right. \\
& \left. - \frac{1}{2M_N} (\boldsymbol{\sigma}_2\cdot\boldsymbol{k}) \left[(A+B)\frac{\boldsymbol{k}^2}{m_\pi^3} + D\frac{1}{m_\pi} \right] \right\} \\
& \cdot (\boldsymbol{\tau}_1\cdot\boldsymbol{\tau}_2) \frac{1}{\boldsymbol{k}^2 + m_\pi^2} \frac{1}{\boldsymbol{k}^2 + m_\pi^2}
\end{aligned} \tag{A6}$$

REFERENCES

[1] A. Feliciello and T. Nagae, Rep. Prog. Phys. **78**, 096301 (2015).
[2] E. Botta, T. Bressani, S. Bufalino, and A. Feliciello, Riv. Nuovo Cimento **38**, 387 (2015).
[3] G. Garbarino, Nucl. Phys. A **914**, 170 (2013).
[4] C. Chumillas, G. Garbarino, A. Parreño, and A. Ramos, Phys. Lett. B **657**, 180 (2007).
[5] K. Itonaga and T. Motoba, Prog. Theor. Phys. Suppl. **185**, 252 (2010).
[6] K. Itonaga, T. Motoba, and Th. A. Rijken, Prog. Theor. Exp. Phys. **2018**, 113D01 (2018).
[7] W. M. Alberico, A. De Pace, M. Ericson, and A. Molinari, Phys. Lett. B **256**, 134 (1991).
[8] M. Kim et al., Phys. Rev. Lett. **103**, 182502 (2009).
[9] H. Bhang et al., J. Korean Phys. Soc. **59**, 1461 (2011).
[10] M. Agnello et al., Phys. Lett. B **685**, 247 (2010).
[11] M. Agnello et al., Phys. Lett. B **701**, 556 (2011).
[12] M. Agnello et al., Phys. Lett. B **738**, 499 (2014).
[13] E. Botta, T. Bressani, S. Bufalino, and A. Feliciello, Phys. Lett. B **748**, 86 (2015).
[14] A. Ramos, E. Oset, and L. L. Salcedo, Phys. Rev. C **50**, 2314 (1994).

[15] E. Bauer and F. Krmpotić, Nucl. Phys. A **739**, 109 (2004).
[16] E. Bauer and G. Garbarino, Nucl. Phys. A **828**, 29 (2009).
[17] E. Bauer and G. Garbarino, Phys. Rev. C **81**, 064315 (2010).
[18] S. Shinmura, Prog. Theor. Phys. **97**, 283 (1997).
[19] J. Fujita and H. Miyazawa, Prog. Theor. Phys. **17**, 360 (1957).
[20] Th. A. Rijken and V. G. J. Stoks, Phys. Rev. C **54**, 2869 (1996).
[21] Th. A. Rijken, Phys. Rev. C **73**, 044007 (2006).
[22] Th. A. Rijken and Y. Yamamoto, Phys. Rev. C **73**, 044008 (2006).
[23] Th. A. Rijken, M. M. Nagels, and Y. Yamamoto, Prog. Theor. Phys. Suppl. **185**, 14 (2010).
[24] M. M. Nagels, Th. A. Rijken, and Y. Yamamoto, Extended soft-core Baryon-Baryon Model ESC08. I. Nucleon-Nucleon Scattering . Available at: http://nn-online.org/eprints/pdf/16.01.pdf, (last accessed date: August 28, 2022).
[25] M. M. Nagels, Th. A. Rijken, and Y. Yamamoto, Extended soft-core Baryon-Baryon Model ESC08. II. Hyperon-Nucleon Scattering. Available at: http://nn-online.org/eprints/pdf/16.02.pdf, (last accessed date: August 28, 2022).
[26] M. M. Nagels, Th. A. Rijken, and Y. Yamamoto, Phys. Rev. C **99**, 044002 (2019).
[27] M. M. Nagels, Th. A. Rijken, and Y. Yamamoto, Phys. Rev. C **99**, 044003 (2019).
[28] Th. A. Rijken, GESC18 Two- and Three-body YNN Potentials, Λ N, Σ N, Ξ N G-matrix Application. Available at: http://nn-online.org/eprints/pdf/20.03.pdf, (last accessed date: August 28, 2022).
[29] B. A. Loiseau, Y. Nogami, and C. K. Ross, Nucl. Phys. A **165**, 601 (1971).
[30] T. Ueda, T. Sawada, and S. Takagi, Nucl. Phys. A **285**, 429 (1977).
[31] R. H. Dalitz and F. Von Hippel, Phys. Lett. **10**, 153 (1964).
[32] J. J. J. Kokkedee, *The Quark Model* (Benjamin, New York, 1969).
[33] M. M. Nagels, Th. A. Rijken, and Y. Yamamoto, Phys. Rev. C **102**, 054003 (2020).
[34] H. Kleinert, Fortschr. Phys., **21**, 1 (1973).
[35] N. K. Glendenning, *Compact Stars: Nuclear Physics, Particle Physics, and General Relativity* (Springer, Berlin, 1997), Astronomy and Astrophysics Library.
[36] H. Outa et al., Nucl. Phys. A **754**, 157c (2005).
[37] B. H. Kang et al., Phys. Rev. Lett. **96**, 062301 (2006).
[38] Y. Sato et al., Phys. Rev. C **71**, 025203 (2005).